Chapter 3
The Organic Rankine Cycle

As already discussed in Sect. 1.6, the energy conversion plants based on the steam Rankine cycle guarantee high levels of efficiency (40–50 %) and are characterised by good thermodynamic qualities in cases where the useful power is high (generally, we are talking of hundreds of MWe), so as to justify the costs of the plant incurred by the elevated cycle pressure (150–300 bar), the high maximum temperatures (500–700 °C), all the complexity of the plant layout (numerous regenerators) and of the primary movers (turbine expander).

The current industrial interest in energy saving, in the use—where possible—of renewable energy and in heat recovery, necessitates the use of highly efficient thermodynamic tools: these should be suitable for the variety of heat sources available and for varying sizes of power supply.

For example, a significant quantity of waste heat is produced by industrial processes, at relatively high temperatures (200–600 °C), frequently available as the sensible heat of gas flows or from vapour condensation (of pure or multicomponent vapours). In such cases, the steam may be thermodynamically and economically inadequate.

In Italy, for instance, a recent study has estimated that, just for the waste heat recovery using Organic Rankine Cycles (ORC) technology of the size of 0.5–5 MW for the sectors of metalworking, cementmaking and glassmaking, there is a potential installed power of around 130 MW, corresponding to a total of between 640 and 1,025 GWh of producible electricity per year.

By way of a further example, in the sector of renewable energy, several forecasts agree on the enormous potential for exploiting the geothermal energy resources of the planet. The geothermal resources often consist of multicomponent fluids and vapours, also with significant quantities of incondensable gases, which could render them both difficult and inappropriate for use directly in steam cycles. In such cases, the use of organic fluid engines could be the only valid alternative.

In general, therefore, wherever the use of steam is unsatisfactory due to low efficiency levels or for the excessive plant costs, systems based on the use of Rankine cycles that use working fluids other than steam could well be the answer.

C.M. Invernizzi, *Closed Power Cycles*, Lecture Notes in Energy 11,
DOI 10.1007/978-1-4471-5140-1_3, © Springer-Verlag London 2013

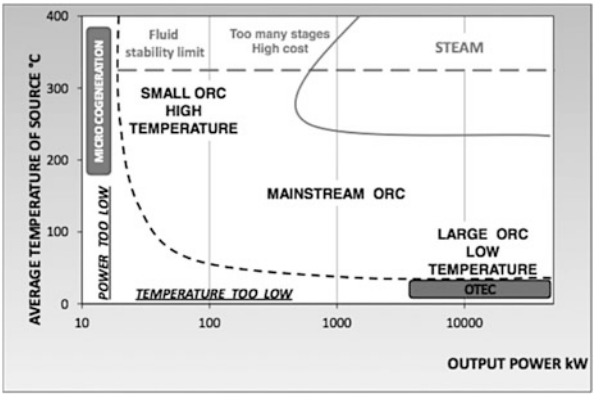

Fig. 3.1 Fields of employment for the Rankine cycle engine: steam cycles and Organic Rankine Cycles (from author [1])

Such engines have been developed and are still the object of intense research and development projects. The fluids used tend to be organic fluids and the thermodynamic cycles that utilise them are called ORC.

For special applications, the organic fluids give indubitable advantages over the use of steam, but, on the downside, they are sometimes costly, are characterised by poor thermal exchange properties and involve potential risks to safety (inflammability) and health (toxicity).

Figure 3.1 represents in a synthetic but approximate manner the field of employment, in terms of temperature and power, for heat engines using both steam and organic fluid. Steam has practically no rivals in applications requiring great power levels (higher than 500–1,000 kW) and at medium–high temperatures (above 200–250 °C). For lower power levels, the steam turbine is usually too expensive. Organic fluids have a heat stability limit that restricts their use to maximum temperatures of 300–400 °C. Temperatures that are excessively low (below 70–100 °C) render the costs of the heat engine so high that it is often inadvisable to use them. Unless, that is, the power levels are particularly high (as in the case of OTEC systems). Very low power levels (below a few dozen kWe, typical in micro-cogeneration systems) mean high costs for the organic fluid engine and, consequently, it becomes at present often uneconomic.

In any case, the range of potential applications for the ORC, at low and medium–high temperatures, is vast and interest in the technology is growing rapidly. Growth potential is particularly strong in all those sectors of primary generation and cogeneration (including the domestic field, within the range of a few kW); in systems using biomass (both residual and in the form of energy crops), when there are difficult fuels involved (syngas, flare gas, etc.); in the solar thermodynamic sector; in the numerous cases of heat recovery (from industrial processes, from gas turbines, from reciprocating ICE, in plants for re-gasification of natural gas, etc.) and in the exploitation of geothermal sources and in OTEC systems.

There are now commercially available turbomachines or expanders for ORC with power levels below 50 kW and ever smaller organic fluid engines are being proposed with scroll expanders. The greatest challenge for the industry of ORC systems today, especially for cases of low temperature and low power levels, is not so much the thermodynamic efficiency, which is potentially already very good, but the reduction of costs. In this sense, the synergy that now exists between the HVAC sector and the companies that develop ORC systems appears very promising, although the air-conditioning industry has developed and continues to develop refrigerating fluids that sometimes appear—from a strictly thermodynamic point of view—far from optimal for heat engines.

In this chapter, we shall discuss the principal characteristics of organic fluids and the Rankine cycles that can be made using them, with some real examples of engines.

3.1 A Brief History of the Organic Rankine Engines

The ORC, as mentioned above, is a Rankine cycle that does not use steam as its working fluid, but another fluid, generally an organic fluid.[1]

William J.M. Rankine developed a complete theory of the steam engine in his famous manual of 1859 [2], but, as early as 1825–1826, Thomas Howard had made an engine using "alcohol" or "ether" as working fluid. Various authors refer to it and describe it ([3, p. 217], [4, p. 599], [5, p. 644]). In [5] it says

> The intention of the inventor of this engine, was the employment of alcohol or ether, as a motive power, on the ground of their exerting a much greater expansive force than steam, at similar temperatures.

It appears that the engine, with a design power of 24 hp (about 18 kW), worked for a brief period in Rotherhithe, Surrey, UK.

The British journal The Engineer, on 9 January 1885,[2] contains an article that describes the results of a test carried out by a commission of the United States naval engineers on a launch engine, which used as its working fluid a solution of water and methyl alcohol[3] (with 5–15 % methyl alcohol): a binary vapour engine.[4]

---

[1] By organic fluid or compost we mean any compost, not necessarily present in living organisms, containing a significant quantity of carbon.

[2] A great deal of interesting information and anecdotes about unusual working fluids and much else can be found in "The Museum of Retro Technology". Available at http://www.douglas-self.com/MUSEUM/museum.htm. (cited May 27, 2012)

[3] The methyl alcohol, known also as methanol, is a well-known alcohol fuel. Its chemical formula is CH_3OH, its boiling point is 65 °C and at 25 °C it has a vapour pressure of 0.17 bar. The critical temperature is 239 °C and the critical pressure 81 bar.

[4] Here, the term "binary" refers to the working fluid, obtained by mixing two compounds. In its modern usage, the term "binary" identifies an engine with two working fluids that are distinct and physically separate from each other, each operating at a different temperature.

The commission made a rigorous comparison with the performance of the same engine when using steam. This showed, for the binary vapour engine, a specific fuel consumption of 5.07 lb of coal per hourly horsepower, compared to a specific consumption of 5.76 lb of coal per hourly horsepower in the case of the steam engine. It is worth reporting the conclusions of the commission:

> although it is not clear in the minds of the Board how a vapour requiring less heat in its production can give up more of its heat in the production of power than another vapour under like conditions containing a greater quantity of work, yet, accepting the result of trials as being absolutely correct, it would be well to see what this saving costs.

Given the market price of methyl alcohol and the excessive leakage of fluid from the engine, the economic results were decidedly unfavourable for the binary vapour engine. A subsequent engine, of greater power (150 hp, compared to the 10 hp of the prototype), did not work at all, due to the distillation of methyl alcohol in the boiler and the uncontrollable leakage of nauseating fumes.

Around 1850, Du Tremblay, an engineer from Lyon, created a binary heat engine with steam for the engine at high temperature and with "ether" (probably diethyl ether,[5] a compound that is much more volatile than water) for the engine at a lower temperature [6, p. 131]. After evaporation in the boiler and expansion in the cylinders, the steam released its thermal energy of condensation to the second engine, causing the evaporation of the ether which, expanding in another cylinder, produced further work. In this way, he created a real binary cycle (see Chap. 5).

The engine was installed in several passenger ships, but, following an explosion caused by the ether, at the port of Bahia, South America, in 1856, the construction of steam-ether binary motors was interrupted.

Towards the end of the nineteenth century, some small boats were made with engines that used boiling petrol in place of steam for the power system. The most wellknown of these were those built by Frank W. Ofeldt (the "naphtha launches"), which entered production from 1897. The working fluid for the engine was naphtha,[6] which was also used as lubricant for the moving parts and as fuel for the evaporation of the working fluid. These launches enjoyed a moderate commercial success thanks to the existence, in the United States, of a law obliging the presence of a qualified engineer aboard whenever there was a steam engine present. The law did not apply to boilers using other types of vapours.

However, it was not until the twentieth century that the ORC was developed intensively. In the sector of thermodynamic conversion of solar energy, Tito Romagnoli, an Italian, developed several Rankine engines between 1923 and

[5]The chemical formula for diethylether, which is extremely inflammable, is $CH_3–CH_2–O–CH_2–CH_3$, and its boiling point is 34 °C; at a temperature of 25 °C, the vapour pressure is 0.71 bar. The critical temperature is 194 °C and the critical pressure 36.4 bar.

[6]The term "naphtha" is generally used to identify mixtures of hydrocarbons. Naphtha is often used as a feedstock for the production of gasoline.

1930: one, around 2 hp (about 1.5 kW), with methyl chloride[7] as its working fluid. He used fixed solar collectors, probably flat, without concentration [7, 8].

Between 1961 and 1962, Harry Zvi Tabor and Lucien Bronicki built various Rankine engines with monochlorobenzene[8] at 140–150 °C, with power from 2–10 kW [9].

Some solar pumping systems were developed, in the years 1977–1978, with engines using refrigerant 113[9] from 20–40 kW [9, 10, p. 639]. Solar Rankine engines using toluene,[10], with parabolic dish collectors, and a maximum temperature of 400 °C, were made between 1983 and 1984 with power from 25–100 kW.

In 1967, in the Soviet Union on the Kamchatka peninsula, what is generally considered to be the first geothermal binary cycle was installed. The working fluid was the refrigerant 12[11] and the engine had a gross power of 680 kW. The heat source was geothermal water at low temperature (80 °C) [11, p. 519].

The ORC started to be taken into serious consideration in the late 1980s, also for use as devices for the dynamic conversion of solar energy in space, since, unlike the closed Brayton cycles; by functioning at lower maximum temperatures (400 °C compared to the 750–800 °C necessary for closed gas cycles, see Sect. 1.7), they enabled the use of lighter and more conservatively designed concentrators, guaranteeing high performance at concentration ratios below 500, and, at the same time, allowing numerous materials to be employed in the heat storage [12].

By 1981, there were 2,150 Rankine engines with 16 different working fluids, made by about 20 different engine manufacturers. In terms of the number of engines and operating time, the leading manufacturer of Organic Rankine engines at the time had made 2,000 of them, with a total of 18,000,000 operating hours, using trichlorobenzene as the working fluid (see [13]).

Starting with the early attempts (at the end of the nineteenth century) and the organic fluid engines that were built up to the 1970s and 1980s, there have been numerous models. Far more than those briefly listed above: the references [7, 9, 13] give a fairly complete description of them. This brief overview, though, makes it clear how the initial fluids employed were those of the refrigeration industry: not only the organic fluids in the strict sense, but also sulphur dioxide (Henry E. Willsie, in 1904, built two solar power plants with SO_2 1 of 6 hp and 1 of 15 hp) and

[7] The methyl chloride, or chloromethane, with a chemical formula CH_3Cl, has a boiling point of −24.2 °C.

[8] Chemical formula C_6H_5Cl, boiling point 131.76 °C, critical temperature 359.25 °C and critical pressure 45.2 bar

[9] 1,1,2-trichloro-1,2.2-trifluoroethane, with boiling point of 47.7 °C

[10] Toluene, or methylbenzene, with chemical formula $C_6H_5CH_3$. Boiling point at 110.4 °C, critical temperature 318.6 °C and critical pressure 41.08 bar

[11] Dichlorodifluoromethane, CCl_2F_2. Boiling point −29.8 °C.

ammonia (for example, the Campbell engine, in 1891). In the first machines, the expander used was mainly volumetric; the turbine was introduced later. There have been numerous solar applications, sometimes resorting to concentration collectors, mostly flat collectors, at low temperatures and with modest power levels. In some cases, the natural salt gradient of the so-called solar ponds was exploited.[12]

The Italian School

Italy has a long tradition in the development of heat engines based on ORC. The studies and the models of the engineer Romagnoli (between 1923 and 1931) have already been mentioned. It is also worth recording those proposed by Prof. Mario Dornig[13] of the Institute of Technical Physics at the Polytechnic of Milan, in the years 1918–1922 (see [14]) and, subsequently, those of Prof. Luigi d'Amelio,[14] professor at what was then the Regio Istituto Superiore d'Ingegneria of Naples, who (see [8]) dedicating himself to the use of solar energy for raising water for agricultural uses in Libya, made detailed studies of an engine using vapours of ethyl chloride.[15] The vapour expansion was ensured by an impulse single-stage turbine, and the working fluid chosen was methyl chloride because, among other things, it meant that the rotor could be made with a peripheral speed lower than 100 m/s, which was then considered to be the prudent top speed. The temperatures of evaporation and condensation were 40 °C and 23 °C, respectively, with a turbine shaft power of around 6 hp (4.5 kW). On the basis of these studies, he then built a pilot plant of 11 kW, in 1940, on the Island of Ischia, where it could use the heat of the local thermal springs. The results were good; however, a second plant of 250 kW, finished in 1943, never went into operation.

A solar engine, at low temperature (about 100 °C) and operating with sulphur dioxide, was designed in the early 1930s by Daniele Gasperini (1895–1960), an

[12] A solar pond is a vast area of salt water which, due to the favourable salt gradient, behaves as a large flat solar collector of thermal energy. A solar pond can be used for a variety of applications, amongst which is the generation of electricity.

[13] Born in Florence in 1880 to parents originating from Trieste. Having graduated in Civil Engineering at Rome in 1904, he moved to Munich, where, in 1911, he obtained his doctorate in Thermal and Mechanical Science. Returning to Italy, in 1917 he obtained the professorship in Fluid Machinery at the Polytechnic of Milan, which he held until his retirement. (1951). He died on 12 November 1962.

[14] Born in Naples on 1 June 1893, he was a professor at the University of Naples and headed the Institute of Thermal, Hydraulic and Agricultural Machinery until 1963. He died in Naples on 1 December 1967.

[15] Ethyl chloride, or chloroethane, has the chemical formula $CH_3–CH_2Cl$, a boiling point of 12.35 °C, a critical temperature of 187.25 °C and a critical pressure of 52.7 bar.

artisan and refrigeration expert from Rovereto (Trento).[16] During his work in Libya, he collaborated with Giovanni Andri to build the first engine model, exhibited at the fair of Tripoli in July 1936. After the Second World War, Gasperini continued to develop his idea and, with the collaboration of Ferruccio Grassi (1897–1980), an engineer from Lecco, he designed and built a solar pump for raising water from below ground, called SOMOR, after the name of the company that built it (SOcietá MOtori Recupero—Company of Recovery Engines—for solar heat and waste heat), exhibited at the first world fair on solar energy, held at Phoenix, Arizona, in 1955 [15].

However, the real Italian School, which significantly and systematically contributed to the development and study of Rankine engines using organic fluid appeared during the second half of the 1960s at the Polytechnic of Milan. Its founder was Prof. Gianfranco Angelino,[17] with Prof. Mario Gaia and Prof. Ennio Macchi, first as his pupils, then as colleagues and friends.

Between 1976 and 1984, the Polytechnic group designed and contributed, with the financial backing of various institutions and private companies, to the realisation of 14 ORC engines, from 3 to 500 kW, to use various heat sources (solar energy, geothermal fluids, industrial waste heat, fossil fuels) [16]. Among these, we should note the following for their peculiarity:

- Several small engines using perchloroethylene[18] (from 3 to 12 kW) at low temperature (from 75 °C to 83 °C, with corresponding evaporation pressures of 0.235–0.306 bar), in which the working fluid was chosen in order to give good turbine design.

[16] In the newspaper The Deseret News—November 15, 1951 (the oldest daily newspaper published in the state of Utah, at Salt Lake City)—there can be read the following brief but curious note:

> The Sun Could Supply Electricity, by A. De Montmorency New York, November 14—A new Italian invention will permit each house to generate its own electricity without any expense of fuel, simply by using the sun's energy. A dispatch from Milan to informations of Madrid reported that Prof. Mario Dorning of that Lombardian city had built with the help of Daniel Gasperini, an engineer, a solar engine capable of producing 10 kilowatt-hours daily. Three such machines have been sent to Egypt for a tryout.

[17] Born in Naples on 18 October 1938. He graduated with full honours in 1962, discussing his thesis on "Prestazioni degli effusori a spina nei propulsori a razzo". In the same year that he graduated, he won an AGARD scholarship for a specialisation course in Experimental Aerodynamics at the Centre de Formation en Aérodynamique Expérimentale, Von Kármán Institute, in Belgium. In 1963 he was awarded his diploma with distinction and received the Theodore Von Kármán prize, which was reserved for the best student of each year. From 1973 to 2009 he was full-time professor in Machinery at the Polytechnic of Milan. He was director of the Machinery Section at the Department of Energy at the Polytechnic of Milan and, for many years, director of the research doctorate in Energy. He died on 9 May 2010.

[18] Perchloroethylene, or tetrachloroethylene, $Cl_2C{=}CCl_2$ is an excellent solvent of organic substances, which is not particularly volatile and is non-inflammable. For these reasons, it is widely used these days in dry cleaning. It has a boiling point of 121.1 °C

- An engine of 500 kW with refrigerant 113,[19] in which a working fluid was chosen that had a critical temperature and molecular complexity that would guarantee an efficient cooling of the heat source (a geothermal fluid).
- Two high temperature (280 °C and 340 °C) perfluorocarbon engines,[20] of 45 and 25 kW, designed to give high efficiency, with a multistage turbine and a demanding regenerator.
- A cogeneration engine with dichlorobenzene,[21] with condensation temperature at 80 °C (condensation pressure 3.5 kPa) and of 100 kW with a 3,000 rpm turbine and a direct-drive turbo-alternator.

Up until the end of the 1980s, the organic fluid engines were prototopical machines, or almost, with an extremely limited market,[22] whilst, today, the use of ORC is expanding rapidly and the basic technology is wellknown. The most common applications have been in the biomass and geothermal sectors, whilst the biggest margin for growth is forecast in the fields of heat recovery and solar thermodynamics (also, in principle, in OTEC plants). In Europe alone, there are now around 200–230 plants operating with organic fluid engines: 80 in Germany, around 70 in Italy and 30 in Austria.

This brief historical overview of the use of organic fluids as working fluids in the energy conversion sector would not be complete without citing the profound studies carried out between the end of the 1950s and the early 1970s into the use of organic fluids in nuclear reactors: the organic-cooled and moderated reactors (OCMR). The abundance of hydrogen in the molecule of organic fluid guarantees excellent moderating capabilities (comparable to those of water) but with a series of advantages for the organic refrigerants with respect to water: vapour pressure is very low at high temperatures, excellent compatibility with carbon steel and low induced radioactivity. Furthermore, their physical properties are wellknown and the cost of the fluids relatively modest. If heavy water were used as the moderator, then, in principle, even natural uranium could be used as fuel. On the downside, the decomposition induced by the temperature and the radiation, together with the relatively low heat exchange capabilities and the inflammability, represent important negative characteristics that discourage the practical use of organic fluids as coolants

[19] 1,2-Dichlorotetrafluoroethane, $ClF_2C–CF_2Cl$, boiling point 3.43 °C, critical temperature 145.75 °C, critical pressure 32.37 bar.

[20] One with Flutec PP3, perfluoro-1,3-dimethylcyclohexane, C_8F_{16}, boiling point 102 °C, critical temperature 241.55 °C and vapour pressure 4.8 kPa at 25 °C; the second with Flutec PP5, perfluorodecalin, or perfluoronaphtalene, $C_{10}F_{18}$, boiling point 142 °C, critical temperature 292 °C and vapour pressure 0.88 kPa at 25 °C

[21] 1,4-Dichlorobenzene, $C_6H_4Cl_2$, boiling point 174 °C

[22] A notable exception was (and continues to be after 40 years) a small generator for generating energy in remote places, called the Remote Power Unit: made with power levels between 600 W and 4 kW, it is very widespread.

in nuclear reactors. The fluids under study were various polyphenyls,[23] with high boiling points (300–400 °C) and critical temperatures of around 600 °C. Besides the research carried out in the United States, similar studies were undertaken in Canada and in the ex-Soviet Union and there was even a detailed Italian project (Progetto Reattore Organico) between 1960 and 1970.

3.2 The Characteristics of Candidate Working Fluids According to the Applications

Engines operating according to a Rankine cycle, with an organic working fluid, generally with a high molecular mass, present characteristics that make them extremely interesting for applications at medium-low temperatures and relatively low power levels (maximum power of a single engine in the order of several MW, at most). The reasons behind the use of fluids other than steam in Rankine cycles are, primarily, thermodynamic and linked to a well-designed expander, usually a turbine. In fact, the choice of an appropriate working fluid will satisfy a variety of needs:

- Fluids with different critical parameters (temperature and pressure) assure that configurations of the thermodynamic cycle become possible to be inaccessible in the state diagram of water, for instance, supercritical cycles even at low maximum temperatures.
- Even where there are great ratios between the temperature of the heat source and the temperature of the cold well, efficient thermodynamic cycles can be achieved with a relatively simple plant set-up and perhaps with one expansion stage, thanks to the regeneration that occurs with a de-superheating of the vapour at the turbine outlet and without having recourse to vapour extraction.
- The turbine requires, for the most part, modest peripheral speed and condensation is avoided during the expansion. The turbine, though, often has supersonic flows with high expansion ratios.
- The choice of fluids, influencing the volumetric flows, permits turbine optimisation for any power level.
- The pressure levels (and the expansion ratios) between the various components may be chosen with a certain freedom, independently of the temperature levels of the heat source and the cold well (for example, low temperatures may be associated with high pressures and high temperatures with low pressures).

The final choice of the working fluid must, inevitably, be influenced by safety and financial considerations. Thus, it is generally the result of a reasonable compromise between the necessary and the desirable characteristics of working fluids in

[23] *Ortho-*, *meta-* and *para*-terphenyls ($((C_6H_5)_2C_6H_4)$) in mixtures. A prototype of a commercial reactor, of 45.5 MWt, was made anyway (under a project of 1956 and the reactor was operational from 1963 to 1966) in Ohio in the USA: the Piqua OMR plant [17].

Rankine power systems: primarily, adequate thermo-physical and thermodynamic properties, compatibility with the materials and the limits of thermal stability of the fluid, the health and safety characteristics, the fluid's availability and its cost. The thermo-physical properties and characteristics of the fluid and their effects upon the performance of the thermodynamic cycle will be discussed in the next section. Here, briefly, we consider the other aspects.

Material Compatibility and Thermochemical Stability Limits

Although organic fluid engines, when designed well, are characterised by an optimal thermodynamic quality, their performance in absolute terms depends on the maximum operating temperatures (see Sect. 1.1).

The choice of the most suitable working fluid passes therefore, necessarily, after an analysis of its thermodynamic behaviour, through the study of its thermal stability and its chemical compatibility, both at room temperature and at operating temperatures, with the materials used in building the plant: those materials used in making the turbines, the heat exchangers and the pumps and used for the tubes, for the seals and for the lubricants. The fluid should be thermally and chemically stable at all operating temperatures, not just in the presence of materials commonly used, but also in the presence of air and water. In any case, the decomposition, which is often inevitable, must occur at a sufficiently slow rate as not to compromise the fluid characteristics and deteriorate excessively the thermodynamic performance of the system.

Tests of various natures have been carried out to establish values of reasonable safety for the maximum operating temperatures. Sometimes this has been done using containing materials for the fluid that are as inert as possible, with the aim of determining the intrinsic molecular stability, sometimes by choosing the materials a priori in order to evaluate their compatibility with the fluid, rather than to investigate the absolute stability. From time to time, different physical properties have been assumed, more or less arbitrarily, as indicators of decomposition in progress (isothermal increases in pressure, formation of carbonaceous deposits, etc.). Catalysis and corrosion can have significant effects on experimental results. Ideally, only accurate tests in experimental apparatus simulating the real behaviour of the engine, both in terms of the materials present and the thermal processes, would be really indicative, but methods which adhere to such measures are very rare.

For this variety of reasons, many of the results available in literature often appear contradictory and only offer a general indication of the thermal stability of the fluid. Figure 3.2 provides values for the maximum temperature of thermal stability, reported by various authors, as a function of the standard binding energy. Whilst the standard binding energy of the atoms that compose the molecule is certainly not the only index controlling the temperature of thermal stability (as we mentioned, the type of materials present, for example, has a major importance), the diagram still gives us useful general indications: the fluids with an aromatic

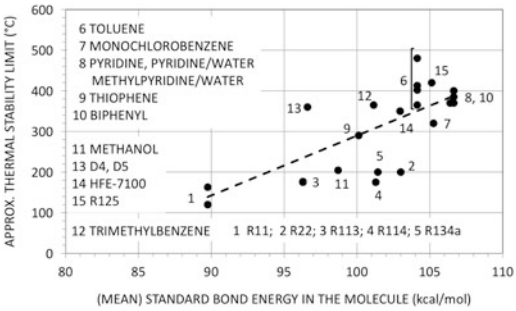

Fig. 3.2 Approximate values of the limit temperature of thermal stability for various working fluids. The temperature values are taken from [12, 13, 18–22]

structure (toluene, pyridine, biphenyl) tend to have the highest thermal stability (about 400 °C); the linear hydrocarbons, under favourable conditions, seem to have limit temperatures of thermal stability of 300–350 °C; and, in general, the cyclical structure (in particular, the aromatic) of the molecule favours stability, more than an open structure. The presence of chlorine significantly reduces the thermal stability (for instance, for monochlorobenzene the maximum temperature of stability is around 300 °C, compared to 400 °C for toluene); by contrast, fluorine atoms, in place of hydrogen or chlorine, significantly raise the thermal stability: for example, refrigerant 125 (pentafluoroethane) and refrigerant 113 (1,1,2-trichloro-1,2,2-trifluoroethane) have limit temperatures of about 400 °C and 200 °C, respectively. The cyclic methylsiloxanes appear to have maximum operating temperatures close to 400 °C and the linear methylsiloxanes 50–100 °C lower. The alcohols seem to be usable up to maximum temperatures of 350–370 °C.

Health, Safety and Environmental Characteristics

A working fluid and its decomposition products ought not to be toxic, carcinogenic or particularly inflammable (or explosive). In fact, inflammability need not be a serious problem provided the appropriate precautions are taken and any potential ignition sources are removed from the critical zones of the plant (setting up the electrical system correctly and putting possible danger points in tubes—the flanges, for example—using fluid sensors and fluid collectors in the case of leakage). Auto ignition is, generally, a bigger problem and so is the risk of reaching explosive concentrations in the air.

From a strictly environmental point of view, the major worries are the ozone depletion potential (ODP), the global warming potential (GWP) and the atmospheric lifetime. For purely environmental reasons, then, numerous cooling fluids with excellent thermodynamic properties have been banned (for example, refrigerant 11, refrigerant 113 and refrigerant 114) and others are due to be phased out between 2020 and 2030. The so-called “natural” fluids, non-halogenated hydrocarbons, ammonia and carbon dioxide, favoured from a strictly environmental point of

view, do not always present adequate thermodynamic characteristics. Among the hydrocarbons, in principle, it is relatively easy to find the most suitable fluid thermodynamically, but there remains the problem of their high inflammability and (for the aromatic hydrocarbons) their toxicity.

Availability and Cost

The fluid should be easy to purchase (maybe from more than one producer) and at a reasonable cost, because this will have a bearing not only on the start-up costs but also on the operating costs through possible leakages and the need for makeup during operation.

3.3 The Thermodynamic Aspects of the Organic Rankine Cycles

Figure 3.3 shows the typical plant layout for an engine with an organic fluid Rankine cycle. The working fluid, which is saturated, superheated or even in supercritical condition, begins its expansion in the turbine from point 4. At the outlet of the turbine, the steam temperature could still be relatively high and, before sending the vapour to the condenser, it could be worth cooling it (from 5 to 6) by means of a recuperative heat exchanger (a regenerator), in such a way as to preheat the liquid originating from the pump prior to sending it to the vapour generator (preheating from point 2 to point 3).

The regenerator is necessary for fluids with high molecular complexity (high σ parameter; see Sect. 2.5). In fact, the expansion of the working fluid, which is isentropic, if ideal, develops from point 4 (corresponding, for example, to saturated vapour) to point 5 in the zone of the superheated vapour (see Fig. 2.5), if σ is positive and, the higher σ is, the less the cooling of the fluid during expansion: assuming that the steam in expansion is similar to a perfect gas, in (2.29) the term C_{p}^{0}/R is equal to $\gamma/(\gamma-1)$ and if γ diminishes, that is, σ increases, once an expansion ratio r_T is set, the gas will cool less (see Sect. 1.7.1 (1.24)).

The ratio C_{p}^{0}/R on which the σ parameter chiefly depends (see Fig. 2.6) is indirectly a function of the number of atoms N making up the molecule. From Fig. 2.6, we see that $\sigma \approx 0$ when $C_{\mathrm{p}}^{0}/R \approx 10$ or, from Fig. 3.4, for a number of atoms $N \approx 5$–10. For $N > 10$, then, the upper limit curve of the fluid on the plane T–S generally has a positive slope and the expansions beginning with saturated vapour invariably take place in the zone of the superheated vapour.

In the condenser in Fig. 3.3, where the fluid passes from the thermodynamic conditions of point 6 to those of point 1, the vapour condensation is normally preceded by a section of de-superheating and in the vapour generator (the primary

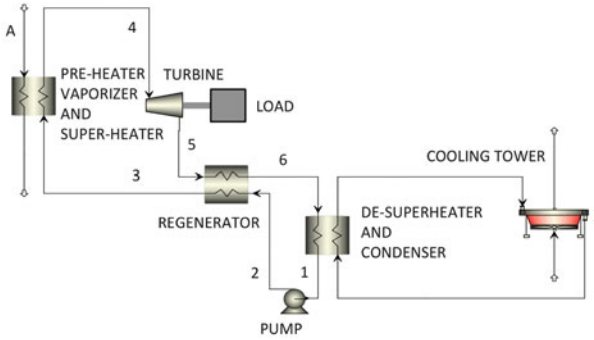

Fig. 3.3 Typical layout for an organic fluid Rankine engine. When the regenerator is not present, point 6 coincides with point 5 and point 3 coincides with point 2

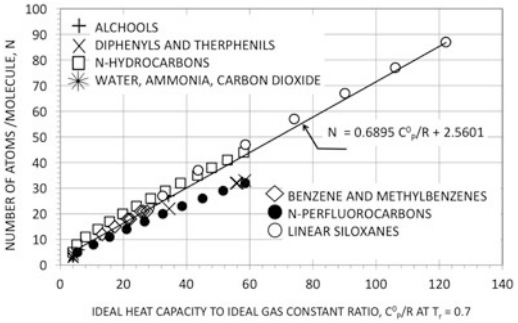

Fig. 3.4 Number of atoms that constitute the molecule, as a function of the ratio C_{P}^{0}/R for certain families of working fluids

heater), a significant percentage of the total heat exchange area is usually dedicated to the preheating phase of the fluid.

If the maximum pressure in the cycle is greater than the critical pressure P_{cr}, the phase change is not present and the fluid, gradually and steadily, passes from the liquid conditions 2 to the gas conditions 4 (crossing the Regions 6 and 7 of Fig. 2.1).

Generally, the heat $\dot{Q}_{\mathrm{in}}$ for the cycle is process heat, available in the form of sensible heat and in Fig. 3.3 the fluid A identifies the heat source fluid.

As already observed (Sect. 2.5), of the numerous thermo-physical properties that characterise each fluid, in fact, only the critical temperature T_{cr} and the molecular complexity (quantifiable by means of the parameter of molecular complexity, σ) play a fundamental role in determining the characteristics of the thermodynamic cycle. Here below, we shall discuss their effects, strictly with regard to the thermodynamic aspects.

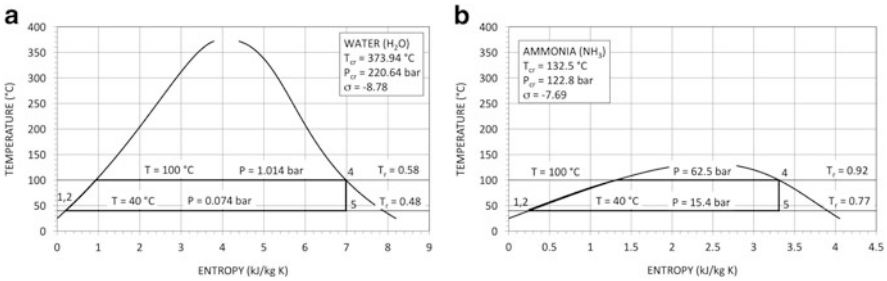

Fig. 3.5 Dependence of the characteristics of the thermodynamic cycle on its position along the limit curve. The two working fluids considered, water and ammonia, are both fluids with low molecular complexity ($\sigma < 0$)

Table 3.1 Some results for the two cycles represented in Fig. 3.5

	Water	Ammonia
Expansion pressure ratio	13.74	4.04
Expansion volume flow ratio	10.31	3.87
Expansion isentropic enthalpy drop (kJ/kg)	384.3	163.2
Turbine exhaust volume flow per unit power ($m^3\ s^{-1}/MW$)	44.87	0.447
Evaporation heat/total heat	0.90	0.67
Preheating heat/total heat	0.10	0.33

The Effect of the Critical Temperature

The critical temperature T_{cr} of the fluid determines the position of the limit curve (and, therefore, of the conversion cycle which is created internally or, for the most part, within it) in the thermodynamic plane, and, having set the temperature levels of practical interest, it establishes in which region of the diagram of the fluid state the thermodynamic cycle will operate. By way of example, Fig. 3.5 reports the limit curves for water and ammonia and, within them, two conversion cycles are traced between the temperatures of 40 °C and 100 °C.

The water cycle uses a region of the state diagram far away from the critical point (at low reduced temperature $T_r = T/T_{cr}$) with low work pressures (prevalently, subatmospheric) and with the introduction of substantially isothermal heat. The ammonia cycle occupies a region of high reduced temperature (close to the critical point) with very high evaporation and condensation pressures and the introduction of heat which is largely not isothermal: see Fig. 3.5 and Table 3.1. The low value of the turbine exhaust volume flow per unit power of the ammonia (due mainly to the high condensation pressure) makes the cycle suitable for high-power engines.

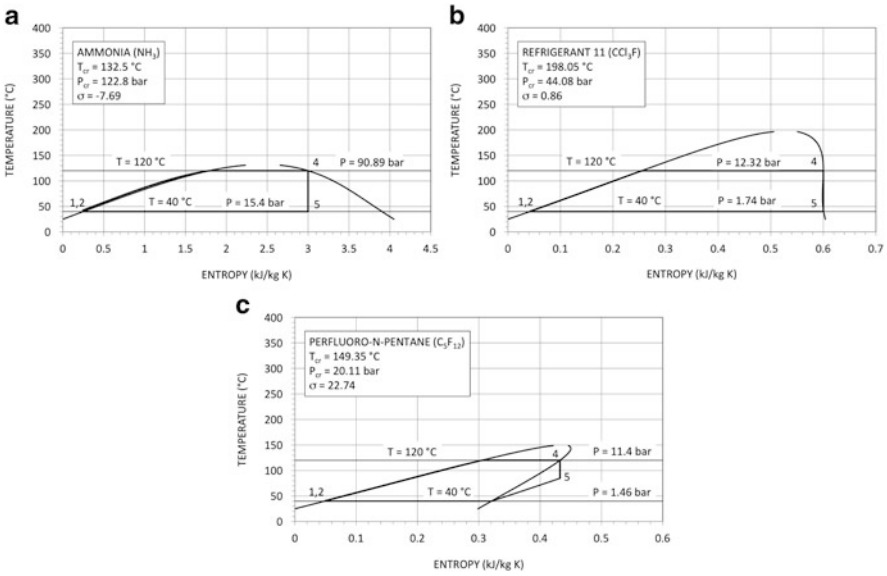

Fig. 3.6 Thermodynamic characteristics of the cycles as a function of the molecular complexity of the working fluid. The three fluids considered have similar critical temperatures, but very different parameters of molecular complexity

The Effect of the Molecular Complexity

The parameter of molecular complexity, σ, determines the shape of the limit curve and, therefore, that of the thermodynamic cycle which is inserted within it. As an example, Fig. 3.6 reports three thermodynamic cycles between the same extreme temperatures (120 °C and 40 °C) but which use three different fluids: the first, ammonia, with a simple molecular structure ($\sigma = -7.69$); the second, refrigerant 11, with a slightly more complex molecule ($\sigma = 0.86$); and the third, *n*-perfluoro-pentane, with a decidedly more complex molecule ($\sigma = 22.74$). It can be noted how, after an isentropic expansion, the first case produces a thick condensation; in the second, the condensation is negligible; in the third, there is a progressive superheating of the vapour as expansion occurs.

The consequences of such thermodynamic behaviour is important for the following reasons:

- For those fluids which do not give rise to any significant condensation during expansion in the turbine, there is no risk of erosion by the drops of liquid, which is a well-known danger in steam plants.
- The thermo-physical reason that keeps the risk of condensation at bay (the great molar heat, linked to the numerous degrees of freedom of complex molecule, that is, a high value of the C_p^0/R ratio; see (2.29)) also tends to make the specific heat of the liquid high and, therefore, its enthalpy, too, with the result that the

Table 3.2 Some results for the thermodynamic cycles of Fig. 3.6

	Ammonia	Refrigerant 11	Perfluoro-*n*-pentane
Expansion pressure ratio	5.88	7.08	7.80
Expansion volume flow ratio	6.13	6.79	10.51
Expansion isentropic enthalpy drop (kJ/kg)	182.25	36.86	18.77
Evaporation heat/total heat	0.46	0.64	0.35

heat is introduced to an appreciable degree also during the preheating phase of the liquid (compare Figs. 3.5a and 3.6a, c and see Table 3.2). This introduction of heat at lower levels than the maximum temperature, whilst penalising the thermodynamic cycle, also makes fractions of thermal energy at low temperature available for use, which, otherwise would have no use within the conversion cycle.

Table 3.2 shows some results for the thermodynamic cycles of Fig. 3.6. The expansion ratios are similar (the critical temperatures of the three fluids considered are, in fact, analogous: they differ only by around 15–20 %). The combined result of the great molecular complexity and the high value of the molecular mass is that the perfluoro-*n*-pentane cools down only slightly following expansion and provides a low specific work (18.77 kJ/kg, compared to a value of 182.2 kJ/kg for ammonia). This modest cooling during expansion of the perfluoro-*n*-pentane makes available an enormous quantity of heat that has been recovered from the regenerator (see Fig. 3.6c): the heat of the de-superheating is 44 % of the value of that of the condensation.

3.4 The Connections Between the Thermodynamics and the Machines

As we have seen and discussed in Sect. 1.6, the good performance of steam cycles is generally linked to a great complexity in the plant layout and in the prime mover (the turbine expander). Such complexity, while perfectly justified in the large thermoelectric power stations, cannot be transferred in practice to stations with more modest power levels (even at the level of a few dozen electrical MW there is a net simplification of the thermodynamic cycle and, often, a sharp drop in the quality of the expander). For power levels lower than several MW both technical and economic considerations suggest that the primary engine should have an internal performance that is not infrequently lower than 50 % and only exceptionally higher than 70 % (adopting multistage turbines with high revs—6,000–12,000 rpm). For power levels of several hundred kW it is not uncommon to have internal performances lower than 30–35 %.

The reason for such modest efficiency lies, firstly, in the high enthalpy drop that characterises the steam cycles (together with the technical and economic limitations linked to the peripheral speed and the number of stages) and, secondly, to the insufficient volumetric flows in the first phases of expansion.

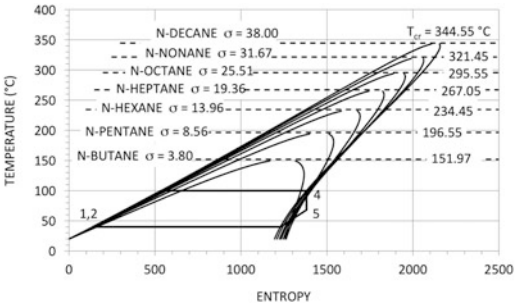

Fig. 3.7 Example of the use of different regions of the thermodynamic plane (reduced) temperature–entropy for the organisation of thermodynamic cycles between the same temperature levels

Having recourse to fluids other than steam (as already shown in the examples above) may bring about a significant reduction in the work of expansion, together with an adjustment of the volumetric flow to the minimum requirements of the turbo-expander. When the power level drops from the MW to just tens or even single kW, the possibility of choosing a fluid other than steam can make all the difference between feasibility and non-feasibility for a plant. The freedom to choose the levels of operating pressure (deriving from the freedom to choose the working fluid) makes it possible to obtain volume flows that are adequate to the turbomachinery.

To illustrate these aspects of interaction (thermodynamics—turbomachinery—heat exchangers), the following example may be useful [16]: consider a homogenous class of organic fluids (in our case, saturated hydrocarbons with a linear structure), whose components have a growing molecular complexity and, consequently, rising critical temperatures (see Fig. 3.7).

Use each of these fluids to make an engine of a given power (100 kW) between temperature levels that are also preset (maximum temperature $T_H = 100\,°C$, minimum temperature $T_C = 40\,°C$; see Fig. 3.7). The first result of such a choice would be the use of regions at different reduced temperature (T/T_{cr}) within the limit curve for the construction of thermodynamic cycles. Other direct consequences would be the reduction of the pressure levels (see (2.20), Fig. 2.3a and Sect. 2.5) and the temperature drop in the turbine with the increase in the molecular complexity (see Sect. 1.7.1 (1.24) and Sect. 3.3). The reduced cooling in the turbine means a growing benefit in the recovery of residual sensible heat in the vapour at the end of expansion by means of a regenerator.

The attendant effects on the thermodynamics of the cycle, the machinery and the regenerator are illustrated in Fig. 3.8a, b, and may be summarised as follows:

- The cycle efficiency tends to grow, if only slightly, as the molecular complexity grows in that, at lower reduced temperatures, the ratio evaporation heat/specific heat of the liquid increases and the preheating phase of the liquid assumes a relatively minor importance. By contrast, it is increasingly important to foresee the regeneration of the residual sensible heat at the turbine outlet, which grows rapidly as the molecular complexity increases (Fig. 3.8b). Only the fluids with a relatively simple molecule (like *n*-butane) can tolerate non-regenerative cycles (Fig. 3.8a).

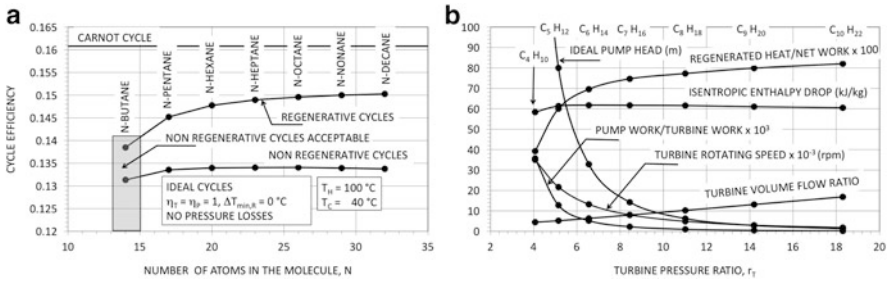

Fig. 3.8 Cycle efficiency and the various characteristics of the cycle and turbine as a function of the molecular complexity of the working fluid (in this figure, the molecular complexity is expressed by the growing number N of atoms, rather than by the factor σ of molecular complexity)

- The turbine pressure ratio grows continuously with the increasing molecular complexity, from 4 (*n*-butane) to about 18 (*n*-decane), causing an increase, albeit modest, in the work of expansion, despite the contrasting effect of the rise in molecular mass (see Fig. 3.8b). As the pressure ratio grows, so does the volume flow ratio (from about 5 to around 20).
- The angular speed of an optimised single-stage turbine decreases continuously as the molecular complexity grows, from 35,000 rpm for *n*-butane to 3,000 rpm for *n*-nonane, down to 1,800 rpm for *n*-decane (see Fig. 3.8b). Likewise, the average diameters of the rotor increase: from about 0.1 m to about 2 m.
- The work (and, therefore, the power) of the pump is fairly high for fluids with a simple molecule (around 4 % of that of the turbine in the case of *n*-butane) but rapidly becomes negligible as the molecular complexity increases. Coinciding with this (see Fig. 3.8b), for the final elements of the class considered (from *n*-octane to *n*-decane) it becomes feasible to eliminate the mechanical compression of the liquid, replacing it with direct feeding from the evaporator via the condenser, located higher up than the evaporator.

The reason for the great variation, as the fluid varies, in the number of revs (and the average diameters) of the turbine, made with just one stage for the sake of simplicity, is to be found in the greatly varying pressures of evaporation and condensation. The condensation pressure passes from 3.77 bar for the cycle with *n*-butane to 5.39 mbar for the cycle with *n*-decane, with a considerable increase in the volume flow at the outlet: from 0.226 to 86.5 m^3/s, respectively, for *n*-butane and for *n*-decane (for an isentropic power of 100 kW). Assuming a specific number of revs $\omega_S = 2\pi N/60 \times \sqrt{\dot{V}_{out}}/\Delta H^{3/4} \approx 0.43$ for the turbine stage at 3,000 rpm with *n*-nonane, with ΔH practically constant (see Fig. 3.8b) and one degree of reaction at the average diameter of 0.11, we get the notable variations in the number of revs and in the diameter mentioned above.

Very similar considerations to those made for the class of *n*-hydrocarbons can be applied to other classes of fluids (for example: chlorofluorocarbons,

perfluorocarbons, aromatic hydrocarbons, siloxanes), and they all highlight the effectiveness of the choice of working fluid in controlling the characteristics of the thermodynamic power cycles.

Component Design: Turbines

As discussed in the example above (but also on the basis of what is illustrated in Sect. 1.7.2 with regard to closed ideal gas cycles), it is clear how the properties of the working fluid play an important role in the design of the turbine. In particular, the size of the enthalpy drop, the mass flow rate and the outlet to inlet volume flow ratio heavily influence the turbine characteristics.

The organic fluids, mostly with a high molar mass, are often characterised by modest values for the enthalpy drop (typically, 10–100 kJ/kg, compared to values of 500–1,500 kJ/kg in the traditional steam cycles), which leads to the possibility of using just one optimised turbine stage, or just a few stages, with a modest peripheral speed and low centrifugal stresses.

According to the cycle characteristics, the volume flow rate ratio may be highly variable: from just a few units for cycles at low temperature or positioned near to the critical point (even supercritical, but with high condensation pressure) up to 1,000 for cycles at high temperature (with a great difference between the maximum temperature and the condensation temperature) and with fluids having high molecular complexity. A large outlet to inlet volume flow ratio over a single stage gives a high number of Mach relative to the rotor inlet and an excessive variation in the blade height. Unusual values in the volume flow ratio often necessitate the exclusion of conventional stages with reaction degrees of 0.5 and have a further consequence in the significant variation in the speed triangles, passing from the root to the tip of the rotor blades.

The real gas effects, especially on the nozzles of the first stage, if the expansion begins near the critical point, may also lead to unconventional geometries of the inter-blade channels.

Figure 3.9b, for example, shows the factor of compressibility Z (see Sect. 2.3) as the expansion ratio varies during an isentropic expansion, with regard to the toluene cycle in Fig. 3.9a. If the expansion begins from a point near the critical point (case with $T_4 = 350$ °C), the compressibility factor Z at the start of the expansion is worth around 0.4 and reaches values of nearly 0.9 only for expansion ratios $r_T \approx 10$; if the temperature at the start of expansion increases, the behaviour of the fluid volume approximates that of the perfect gas at higher pressures (for example, if $T_4 = 400$ °C: $Z = 0.9$ when $r_T \approx 6$ and $Z \approx 0.6$ at the start of expansion). Figure 3.9c shows the area of passage (for unit mass flow of toluene) in the case of isentropic expansion, starting from $T_4 = 350$ °C and $P_4 = 55$ bar. Note how the hypothesis of an ideal gas tends to overestimate significantly the areas, especially the throat area (the minimum value).

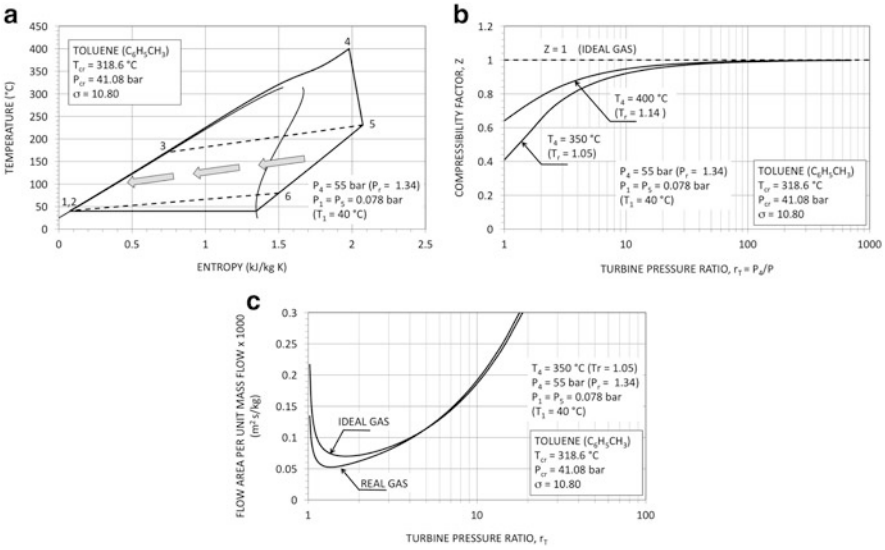

Fig. 3.9 (**a**) Supercritical cycle with toluene in the thermodynamic plane temperature–entropy. The plant layout is that shown in Fig. 3.3. (**b**) Behaviour of the compressibility factor during the isentropic expansion, as the expansion ratio varies. (**c**) Behaviour of the passage area during isentropic expansion for a unit mass flow of working fluid

In general, therefore, since the compressibility factor has a direct influence on the areas of passage for organic fluid cycles, the hypothesis of an ideal gas (with $Z = 1$) or, even more so, of a perfect gas (assuming, too, that C_P stays constant with the temperature; see Fig. 2.4) could prove to be misleading and lead to non-optimal solutions for the turbine.

Component Design: Heat Exchangers

The simplest evaporators to make are usually those of the pool-boiling type, which, thanks to their capacity for storing great volumes of fluid, are also less problematic in the power transitions. Should we need to minimise the fluid inventory (in the case of working fluids that are particularly expensive, for instance), the once-through solution is the most economical, even at subcritical pressures.

In condensers, the use of low integral fins is often a solution for reducing their size, which, otherwise, is penalised by the overall heat transfer coefficients which are modest for the organic vapours that condense (typically, in water condensers, 300–1,200 W/m^2 K for organic vapours compared to 1,500–4,000 W/m^2 K for steam) and for the large sections of passage needed if the turbine discharges at low pressure.

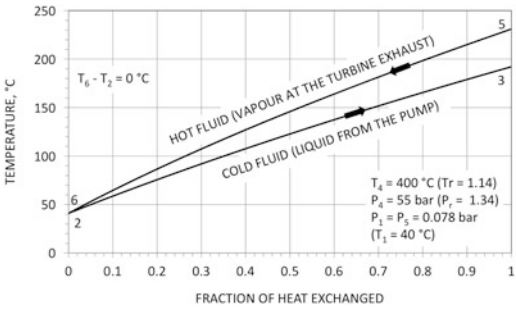

Fig. 3.10 Diagram of the heat exchange for the regenerator (in ideal hypothesis) of the cycle in Fig. 3.9a. Working fluid: toluene

The regenerator is one of the peculiar components to the ORC. In those cycles with high ratios between the maximum and minimum temperatures and for fluids with high molecular complexity, the regenerator can dramatically raise cycle performance, which, however, will then be heavily dependent on the efficiency of the regenerator itself. The best configuration from the thermodynamic point of view would be that which is perfectly countercurrent, although this is difficult to achieve when the volume flows of the two fluids are very different. For the regenerators, just as for the condensers, the presence of a turbine at low revs with a high discharge area (low condensation pressures) may make the positioning difficult for given preset volumes.

Figure 3.10 shows the heat exchange diagram for the regenerator in the toluene cycle of Fig. 3.9a in the case where the minimum temperature difference ($T_6 - T_2$) is null (ideal regenerator). Although the minimum temperature difference between the hot and cold fluids is equal to zero at one extremity (infinite heat exchange surface), the temperature T_3 does not reach the value T_5 anyway because the two fluids (the hot and the cold) have very different specific heat averages: about 1.56 kJ/kg K for the vapour at low pressure, originating from the turbine, and 1.96 kJ/kg K for the liquid originating from the feed pump. This difference in specific heats means that, even in the ideal case, the regenerator suffers from an intrinsic thermodynamic loss, which cannot be eliminated. That said, this will be amply outweighed by the overall thermodynamic benefit due to recovering (if only partially, in the real case) the heat which is ideally available ($H_5 - H_6$) in Fig. 3.10 (which, in the case considered, is 1.16 times the useful work).

Figure 3.11 reports the performances calculated for saturated cycles, with and without regeneration, for several typical working fluids. The parameters assumed for the calculations are given in the figure. The results are indicative of the performances obtainable from ORCs at the maximum temperatures and condensation considered. Several thermo-physical properties of a thermodynamic interest for the fluids under consideration are collected in Table 3.3. As we can see, the working fluids with the high molecular complexity benefit substantially from the regeneration and the performances obtainable are, in this case, close to 27 %, with maximum temperatures of around 300 °C.

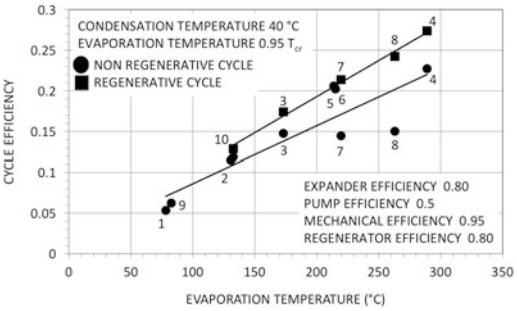

Fig. 3.11 Cycle efficiency as a function of the evaporation temperature for different working fluids and for cycle with and without regeneration. The numbers that identify the various fluids are the same as in Table 3.3

Table 3.3 Some thermo-physical data for possible working fluids in ORCs

No.	Fluid	Critical temperature (°C)	Critical pressure (bar)	Boiling temperature (°C)	Parameter of molecular complexity
1	Propane	96.68	42.48	−42.04	−1.24
2	*n*-Butane	151.97	37.96	−0.5	3.80
3	*n*-Pentane	196.55	33.7	36.07	8.56
4	Toluene	318.6	41.08	110.63	10.80
5	Methanol	239.35	80.84	64.7	−8.85
6	Ethanol	240.85	61.37	78.29	−5.09
7	MM[a]	245.55	19.14	100.52	30.75
8	MDM[b]	291.25	14.4	152.55	45.53
9	HFC 134a[c]	101.3	40.56	−26.07	−3.28
10	HFC 245fa[d]	154.05	36.4	15.3	6.147

[a]Hexamethyldisiloxane
[b]Octamethyltrisiloxane
[c]Hydrofluorocarbon (or refrigerant) 134a: 1,1,1,2-tetrafluoroethane
[d]Hydrofluorocarbon (or refrigerant) 245fa: 1,1,1,3,3-pentafluoropropane

The performance of the cycle with MDM[24] (parameter of molecular complexity $\sigma = 45.53$), for instance, passes from a value of 15 % to 24 % in the case of a cycle with regenerator. Figure 3.12 represents the cycle on the thermodynamic plane temperature–entropy. As the graph makes clear, obtaining a good performance requires a massive regeneration (the heat regenerated is 2.5 times the useful work). Other peculiarities of the cycle are the relatively modest work of expansion (isentropic enthalpy drop is 100 kJ/kg) and the large volumetric expansion ratio (about 900, in the example considered). The modest turbine enthalpy drop is associated

[24]The octamethyltrisiloxane (MDM) is a member of the family of methylsiloxanes fluids, attractive working fluids for organic fluid cycles due to their technical characteristics: they are not toxic, only moderately inflammable and reasonably stable up to 300–350 °C (see [19]).

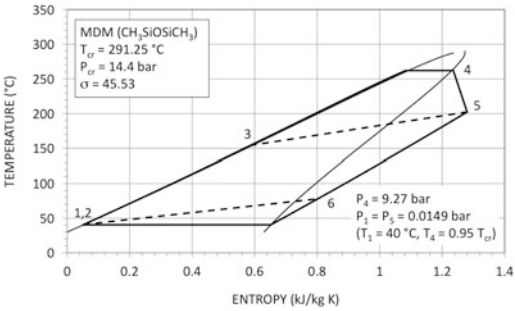

Fig. 3.12 Thermodynamic cycle with MDM in the thermodynamic plane T–S. The cycle performance is equal to 0.24. The parameters assumed for the calculation are those reported in Fig. 3.11

with the high volume flows at the outlet of the turbine. These characteristics are typical of all the working fluids with a molecular complexity similar to that of MDM.

Since most of the current applications use organic fluid Rankine engines principally for heat recovery, we shall discuss various aspects of the thermodynamics of the heat recovery in the next section.

3.5 The Heat Recovery: Basic Thermodynamic Considerations

Figure 3.13 represents a conceptual diagram of a system which consists of one heat recovery heat exchanger and one thermal engine. The engine uses the heat, available at temperature $T_{H,1}$, associated with a hot fluid with mass flow $\dot{m}_H$. In the drawing of Fig. 3.13, the engine uses a heat exchanger to cool the heat source fluid up to the temperature $T_{H,2}$ and converts the thermal power $\dot{m}_H (H_{H,1} - H_{H,2})$ into mechanical power $\dot{W}$. The engine (ideal) works between the temperature T_H ($\leq T_{H,2}$) and the temperature T_C ($\geq T_0$). The thermal power $\dot{Q}_{out}$ is returned to the environment, at temperature T_0, by means of an appropriate heat exchanger.

The mechanical power $\dot{W}$ can be calculated by the exergy balance of Sect. B.1 (B.4), applied to the particular system considered here (in stationary conditions):

$$\dot{m}_H (H_{H,1} - T_0 S_{H,1}) - \dot{m}_H (H_{H,2} - T_0 S_{H,2}) - \dot{W} + \dot{E}_Q - T_0 \dot{S}_G = 0 \qquad (3.1)$$

In which, $\dot{E}_Q = -\dot{Q}_{out} (1 - T_0/T_C)$ (since the thermal power $\dot{Q}_{out}$ at the end of the process is released into the environment at the temperature $T_C > T_0$ assumed constant), $\dot{S}_G$ is the entropy generated in the unit of time in just the recovery heat exchanger (since the heat engine is presumed to be ideal) and $\dot{W}$ is counted with a negative sign since it is produced by the engine (exiting the system, not entering, as per usual in Appendix A).

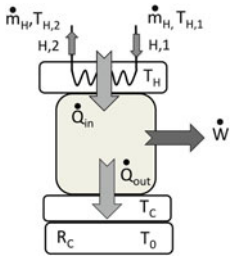

Fig. 3.13 Concept of a heat recovery engine. The heat source consists of fluid at the temperature $T_{H,1}$ which, in the figure, is cooled until the temperature $T_{H,2}$. The engine operates between the temperatures T_H and T_C. Environmental temperature is T_0

The term $\dot{S}_G$ is calculated from the entropic balance (B.3) applied to the heat recovery engine in stationary conditions

$$\dot{m}_H S_{H,1} - \dot{m}_H S_{H,2} + \dot{S} + \dot{S}_G = 0 \tag{3.2}$$

with

$$\dot{S} = (-1)\,\dot{m}_H \frac{H_{H,1} - H_{H,2}}{T_H}$$

From (3.2), we get

$$\dot{S}_G = \dot{m}_H \frac{H_{H,1} - H_{H,2}}{T_H} - \dot{m}_H \left(S_{H,1} - S_{H,2}\right) \tag{3.3}$$

The (3.3) substituted in (3.1) gives

$$\begin{aligned} 0 = {} & \dot{m}_H \left(H_{H,1} - H_{H,2}\right) - \dot{m}_H T_0 \left(S_{H,1} - S_{H,2}\right) \\ & -\dot{W} \frac{T_0}{T_C} \\ & -\dot{m}_H \left(H_{H,1} - H_{H,2}\right) \left(1 - \frac{T_0}{T_C}\right) \\ & -\dot{m}_H T_0 \frac{H_{H,1} - H_{H,2}}{T_H} + \dot{m}_H T_0 \left(S_{H,1} - S_{H,2}\right) \end{aligned}$$

or

$$\dot{W} = \dot{m}_H \left(H_{H,1} - H_{H,2}\right) \left(1 - \frac{T_C}{T_H}\right) \tag{3.4}$$

The thermodynamic efficiency of the conversion of the thermal power $\dot{m}_{\mathrm{H}}\left(H_{\mathrm{H},1}-H_{\mathrm{H},2}\right)$ is therefore $\eta=\left(1-T_{\mathrm{C}}/T_{\mathrm{H}}\right)$.

In general, the heat sources are always fluids that come from industrial processes and from general energy conversion processes (for example, products of the combustion at the outlet of a boiler and at the outlet of an internal combustion engine, gas from a blast furnace) and essentially, from the point of view of the heat transfer, the heat source behaves as (1) a fluid with finite (or equivalent) heat capacity rate $\dot{m}_{\mathrm{H}}C_{\mathrm{P}}$ (for example, liquids, gases or condensing vapours of non-azeotropic mixtures) or as (2) fluids with an infinite heat capacity rate, as, for example, the condensing vapours of pure fluids.

If a heat capacity C_{P} is definable for the fluid, the thermal power yield of the fluid can be written as $\dot{m}_{\mathrm{H}}\left(H_{\mathrm{H},1}-H_{\mathrm{H},2}\right)=\dot{m}_{\mathrm{H}}C_{\mathrm{P}}\left(T_{\mathrm{H},1}-T_{\mathrm{H},2}\right)$. Furthermore, $T_{\mathrm{H},2}=T_{\mathrm{H}}+\Delta T_{\mathrm{min,H}}$, with $\Delta T_{\mathrm{min,H}}$, will represent the minimum difference in temperature (the "pinch point" temperature difference), in the heat recovery exchanger, between the hot fluid (the heat source) and the engine. Then

$$\begin{aligned}\dot{W}&=\dot{m}_{\mathrm{H}}C_{\mathrm{P}}\left(T_{\mathrm{H},1}-T_{\mathrm{H},2}\right)\left(1-\frac{T_{\mathrm{C}}}{T_{\mathrm{H}}}\right)\\&=\dot{m}_{\mathrm{H}}C_{\mathrm{P}}\left(T_{\mathrm{H},1}-T_{\mathrm{H}}-\Delta T_{\mathrm{min,H}}\right)\left(1-\frac{T_{\mathrm{C}}}{T_{\mathrm{H}}}\right)\end{aligned}\tag{3.5}$$

There exists, therefore, once the flow $\dot{m}_{\mathrm{H}}$ has been set, a value of the temperature $T_{\mathrm{H}}=T_{\mathrm{H,opt}}$, corresponding to which the useful power $\dot{W}=\dot{W}_{\mathrm{opt}}$ is the maximum:

$$T_{\mathrm{H,opt}}=\sqrt{T_{\mathrm{C}}\left(T_{\mathrm{H},1}-\Delta T_{\mathrm{min,H}}\right)}\tag{3.6}$$

On the other hand, should we wish to cool the heat source fluid down to the temperature T_0, there exists a limit value for the extractable power (equal to the variation in the physical exergy of the fluid, $\dot{W}_{\mathrm{optimal}}$; see Sect. B.1) obtainable, for example, by calculating the performance from (1.13), assuming $\dot{S}_{\mathrm{G}}=0$:

$$\begin{aligned}\dot{W}_{\mathrm{optimal}}&=\dot{m}_{\mathrm{H}}\left(H_{\mathrm{H},1}-H_{\mathrm{H},0}\right)\left(1-T_0\frac{S_{\mathrm{H},1}-S_{\mathrm{H},0}}{H_{\mathrm{H},1}-H_{\mathrm{H},0}}\right)\\&=\dot{m}_{\mathrm{H}}C_{\mathrm{P}}\left[\left(T_{\mathrm{H},1}-T_0\right)-T_0\ln\frac{T_{\mathrm{H},1}}{T_0}\right]\end{aligned}\tag{3.7}$$

Then, the ratio $\dot{W}_{\mathrm{opt}}/\dot{W}_{\mathrm{optimal}}$, having fixed $T_{\mathrm{H},1}$ and T_{C} and T_0, depends on $\Delta T_{\mathrm{min,H}}$ and is invariably less than 1.0.

Figure 3.14 reports the ratio $\dot{W}_{\mathrm{opt}}/\dot{W}_{\mathrm{optimal}}$ as a function of the temperature difference $\Delta T_{\mathrm{min,H}}$, for certain values of $T_{\mathrm{H},1}$. The ratio between the two powers decreases rapidly with $T_{\mathrm{H},1}$, having set a value of $\Delta T_{\mathrm{min,H}}$. For example, for $\Delta T_{\mathrm{min,H}}=10\ ^{\circ}\mathrm{C}$, the ratio between the pokers passes from 0.49, at $T_{\mathrm{H},1}=400\ ^{\circ}\mathrm{C}$,

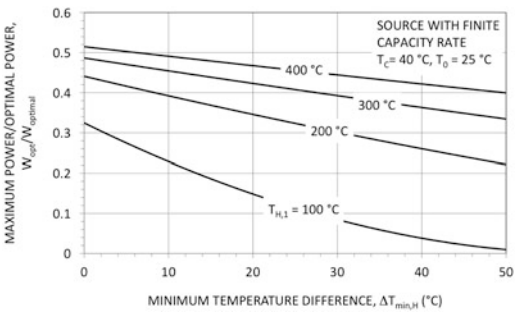

Fig. 3.14 Ratio between the maximum power $\dot{W}_{\text{opt}}$ and the maximum power available $\dot{W}_{\text{optimal}}$, as the minimum difference in the heat recovery machine varies. The scheme referred to is that in Fig. 3.13

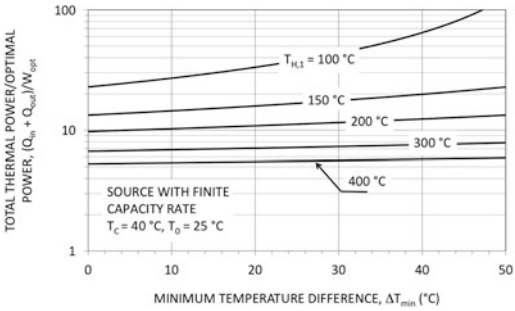

Fig. 3.15 Total thermal power passing through the engine per unit of useful power as the minimum difference in the heat recovery exchanger varies. The scheme referred to is that of Fig. 3.13

to 0.23 when $T_{\text{H,1}} = 100$ °C. Even in the case with $\Delta T_{\text{min,H}}$ null, the maximum power does not equal the maximum power available: $\dot{W}_{\text{opt}}/\dot{W}_{\text{optimal}} = 0.32$ when $T_{\text{H,1}} = 100$ °C and 0.51 when $T_{\text{H,1}} = 400$ °C. This is because the temperature $T_{\text{H,2}}$ is always greater than T_0.

The ratio $\dot{W}_{\text{opt}}/\dot{W}_{\text{optimal}}$ falls with the rise in $\Delta T_{\text{min,H}}$; the lower $T_{\text{H,1}}$ is, the faster this happens: when $\Delta T_{\text{min,H}}$ rises from 0.0 at 50 °C, the ratio passes from 0.32 to 0.01 when $T_{\text{H,1}} = 100$ °C (a fall of 97 %); it passes from 0.51 to 0.40 (a fall of 22 %) when $T_{\text{H,1}} = 400$ °C.

Consequently, it is indispensable that the heat recovery exchanger be designed for a very small pinchpoint temperature difference, especially if the temperature $T_{\text{H,1}}$ is low. Otherwise, the ratio $\dot{W}_{\text{opt}}/\dot{W}_{\text{optimal}}$ will be excessively low.

In any case, the η_{opt} efficiency of thermodynamic conversion of the heat that is recovered will generally be fairly modest (even with $\Delta T_{\text{min,H}}$ null). As a result, the ratio

$$\frac{\dot{Q}_{\text{in}} + \dot{Q}_{\text{out}}}{\dot{W}_{\text{opt}}} = \frac{1}{\eta_{\text{opt}}} + \left(\frac{1}{\eta_{\text{opt}}} - 1\right) \tag{3.8}$$

tends to be high. In (3.8), $\dot{Q}_{\text{in}}$ and $\dot{Q}_{\text{out}}$ represent the thermal power transferred from the heat source to the engine and the thermal power released into the environment by the engine, respectively. The ratio $\left(\dot{Q}_{\text{in}} + \dot{Q}_{\text{out}}\right)/\dot{W}_{\text{opt}}$, which represents the total thermal power passing through the heat exchangers per unit of useful power produced, is shown in graph form in Fig. 3.15 as a function of $\Delta T_{\text{min,H}}$.

The ratio may reach values close to 100, for $\Delta T_{\min}$ excessively high, when $T_{H,1} = 100\ ^\circ C$; it stands at around 20 for $T_{H,1} = 100\ ^\circ C$ and $\Delta T_{\min,H}$ null. When $T_{H,1} = 400\ ^\circ C$, the ratio remains around values of 5–6.

Heat recovery plant are, therefore, characterised by the high cost of heat exchangers per unit of useful energy produced.

In plant engineering there will exist an optimal value of $\Delta T_{\min,H}$ that optimises the cost per unit of mechanical or electrical energy produced: for excessively low values of $\Delta T_{\min,H}$, the ratio $\left(\dot{Q}_{in} + \dot{Q}_{out}\right)/\dot{W}_{opt}$ does diminish, but the surfaces needed for the heat transfer (to guarantee a value which is finite) tend towards the infinite; for an excessively high $\Delta T_{\min,H}$, the η_{opt} conversion efficiency drops and the $\left(\dot{Q}_{in} + \dot{Q}_{out}\right)/\dot{W}_{opt}$ ratio rises and, with it, the cost of generating each unit of energy produced.

The $\dot{W}_{opt}/\dot{W}_{optimal}$ ratio is always lower than the unit on account of three thermodynamic irreversibilities (that is, three lost powers): the irreversibility at the level of the heat recovery exchanger, the irreversibility (the lost work) due to the missing reversible cooling of the source fluid down to environment temperature T_0 and the irreversibility caused by the temperature difference $\Delta T_{\min,C} = (T_C - T_0)$ (see Sect. 1.1 and Appendix C.2. As regards the choice of value to be assigned to $\Delta T_{\min,C}$, see Sect. 1.6.3):

$$\frac{\dot{W}_{opt}}{\dot{W}_{optimal}} = \frac{\dot{W}_{optimal} - \left(\Delta\dot{W}_1 + \Delta\dot{W}_2 + \Delta\dot{W}_3\right)}{\dot{W}_{optimal}} = 1 - \frac{\Delta\dot{W}_1}{\dot{W}_{optimal}} - \frac{\Delta\dot{W}_2}{\dot{W}_{optimal}} - \frac{\Delta\dot{W}_3}{\dot{W}_{optimal}} \tag{3.9}$$

Where a specific heat C_P can be defined for the heat source fluid,

$$\Delta\dot{W}_1 = \dot{m}_H T_0 C_P \left(\frac{T_{H,1} - T_{H,2}}{T_H} - \ln\frac{T_{H,1}}{T_{H,2}}\right) \tag{3.10a}$$

$$\Delta\dot{W}_2 = \dot{m}_H T_0 C_P \left(\frac{T_{H,2} - T_0}{T_0} - \ln\frac{T_{H,2}}{T_0}\right) \tag{3.10b}$$

$$\Delta\dot{W}_3 = \dot{m}_H C_P \left(T_{H,1} - T_{H,2}\right)\frac{T_C}{T_H}\left(1 - \frac{T_0}{T_C}\right) \tag{3.10c}$$

with $T_{H,2} = T_H + \Delta T_{\min,H}$.

The maximum value of the ratio $\dot{W}_{opt}/\dot{W}_{optimal}$, or the maximum value of $\dot{W}_{opt}$ (having set $T_{H,1}$, $T_{H,2}$, T_C and fixed $\Delta T_{\min,H}$), is obtained when the sum of the three fractions of lost work (3.10a), (3.10b) and (3.10c) is least. In correspondence with this minimum, the temperature $T_{H,opt}$ will inevitably be equal to the value supplied by (3.6).

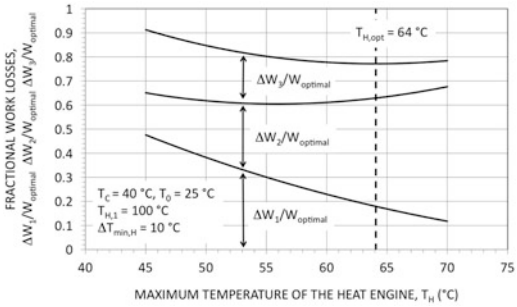

Fig. 3.16 Fractional work losses as a function of the maximum temperature T_H for a system with a recovery heat engine. The concept referred to is that of Fig. 3.13

The ratios $\Delta\dot{W}_1/\dot{W}_{optimal}$, $\Delta\dot{W}_2/\dot{W}_{optimal}$ and $\Delta\dot{W}_3/\dot{W}_{optimal}$ are shown in graph form in Fig. 3.16 as a function of the temperature T_H, for $T_{H,1} = 100\,°C$ and $\Delta T_{min,H} = 10\,°C$. The value of $\Delta\dot{W}_1/\dot{W}_{optimal}$ is 0.48 at $T_H = 45\,°C$ and 0.12 at $T_H = 70\,°C$, as a consequence of the rapid increase in the η efficiency of the thermodynamic cycle of heat conversion. By contrast, $\Delta\dot{W}_2/\dot{W}_{optimal}$ increases by 0.17, for $T_H = 45\,°C$, till 0.56, for $T_H = 70\,°C$, as a consequence of the sudden increase in the thermodynamic loss, associated with the rising temperature $T_{H,2}$ of the source fluid. The sum of the three losses has a minimum that corresponds to the temperature $T_H = T_{H,opt} \approx 64\,°C$.

In general, then, we can state that the global conversion efficiency of the thermal power available (that which is supplied by the hot fluid, assuming that it can be cooled down to environmental temperature) comes from two equally important contributions: the thermodynamic quality of the heat engine's performance and the capacity of the heat engine itself (that is, of the working fluid that is used to make the thermodynamic cycle) to cool as much as possible the heat source fluid.

Strictly speaking, a fourth thermodynamic loss should be taken into account: the irreversible mixing of the heat source fluid with the environment at temperature T_0, at the pressure P_0 and with a fixed composition (the chemical exergy that is not used; see Sects. B and B.1). Generally, though, this final contribution is only modest and can be legitimately overlooked.

The Isothermal Source

If the heat source is at a constant temperature (as, for instance, in the case of condensing vapours of a pure fluid and assuming that we use only the latent heat made available), then $T_{H,1} = T_{H,2}$ and $\dot{m}_H\,(H_{H,1} - H_{H,2})$ represents the power yield of the heat source fluid during condensation. Therefore,

$$\begin{aligned}\dot{W} &= \dot{m}_H\,(H_{H,1} - H_{H,2})\left(1 - \frac{T_C}{T_H}\right)\\ &= \dot{m}_H\,(H_{H,1} - H_{H,2})\left(1 - \frac{T_C}{T_{H,1} - \Delta T_{min,H}}\right)\end{aligned} \tag{3.11}$$

Table 3.4 Some data regarding the fluids considered in Exercise 3.1

Fluid	Critical temperature (°C)	Critical pressure (bar)	Boiling temperature (°C)	Parameter of molecular complexity
Water	373.9	220.4	100	−8.777
CFC 11[a]	198.1	44.08	23.82	0.949
HFC 245fa[b]	154.1	36.4	15.3	6.147
CFC 12[c]	111.8	41.25	−29.79	−1.107

[a]Chlorofluorocarbon (or refrigerant) 11: trichlorofluoromethane
[b]Hydrofluorocarbon (or refrigerant) 245fa: 1,1,1,3,3-pentafluoropropane
[c]Chlorofluorocarbon (or refrigerant) 12: dichlorodifluoroethane

In this case, the maximum useful power and the maximum efficiency of the thermodynamic conversion cycle will be obtained when $\Delta T_{\min,H} = 0.0$ (or $T_H = T_{H,1}$). Thus, if the heat source can be considered isothermal, from a thermodynamic point of view, those cycles are favoured in which the heat is used at the maximum temperature possible, namely, those where the evaporation heat of the working fluid is great compared to the preheating heat. This happens in two different circumstances (see Sect. 3.3): (1) when the thermodynamic cycle is located in the region of low reduced temperatures and (2) when, for given reduced temperatures of evaporation and condensation, a fluid with low molecular complexity is used for the cycle.

Exercises

3.1. With reference to a pressurised water source ($C_P = 4.184\,\text{kJ/kg K}$) with $T_{H,1} = 150\,°\text{C}$ and for the fluids in Table 3.4, the $\dot{W}/\dot{W}_{optimal}$ ratio was calculated for variations in the evaporation pressure. The basic scheme of the thermodynamic cycle is that in Fig. 3.3, without a regenerator. The condensation temperature T_C is assumed to be 40 °C.

In Fig. 3.17, the ratio $\eta_{II} = \dot{W}/\dot{W}_{optimal}$ is represented as a function of the evaporation pressure. The η_{II} parameter can be interpreted as a second law efficiency, according to the definition (1.22), assuming the thermal power $\dot{Q}_{in}$ to be the thermal power available $\dot{m}_H C_P (T_{H,1} - T_0)$.

The evaporation pressure $P_{H,opt}$, which maximises the η_{II} ratio, rises from about 0.66 bar in the case of steam to 36 bar for HCFC 12. If the critical temperature of the working fluid is significantly higher than the temperature $T_{H,1}$, the optimal thermodynamic cycle will be located in the region of the low pressures and reduced temperatures (water and HCFC 11); as the critical temperature of the fluid approaches the value of $T_{H,1}$, the pressure and the reduced temperature of the optimal evaporation rise (HFC 245fa). If the temperature T_{cr} of the fluid is lower than the temperature $T_{H,1}$, the optimal cycle tends to become supercritical (the case of CFC 12).

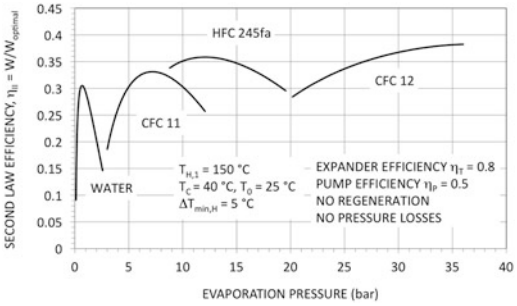

Fig. 3.17 Performance of the ratio between useful power and the maximum mechanical power obtainable from a heat source with variable temperature for different working fluids in thermodynamic cycles

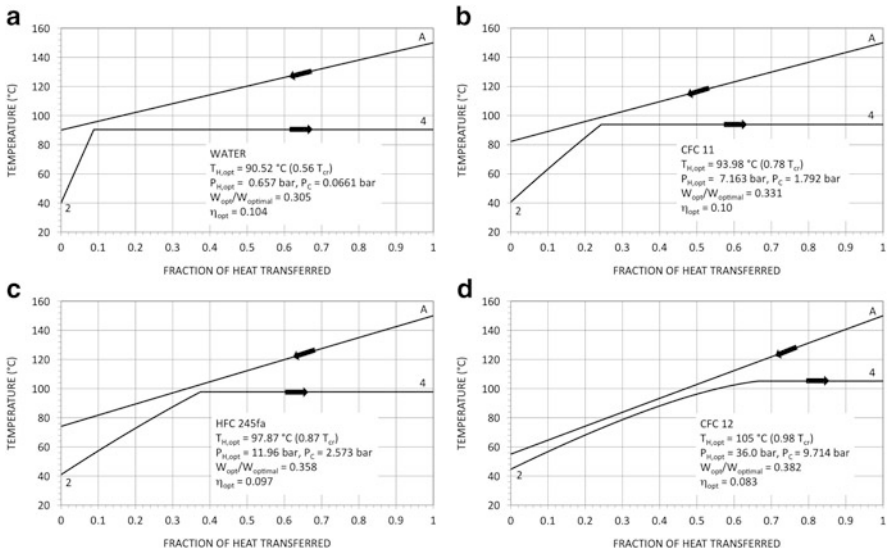

Fig. 3.18 Heat exchange diagrams for the heat recovery exchanger with different working fluids at the maximum power obtainable

The heat exchange diagrams in Fig. 3.18 clearly show how the greater value of the ratio $\eta_{II,opt} = \dot{W}_{opt}/\dot{W}_{optimal}$ is strictly correlated to the greater capacity of the working fluid for cooling the heat source. Although, for example, the steam cycle has an efficiency of 10.04 %, whilst the cycle with HCFC 12 has an efficiency of 8.3 %, the latter (cooling the heat source more) produces a useful power that is 25 % greater than the steam cycle.

Note how the operating conditions of the various cycles differ greatly. In particular, the steam cycle is completely subatmospheric.

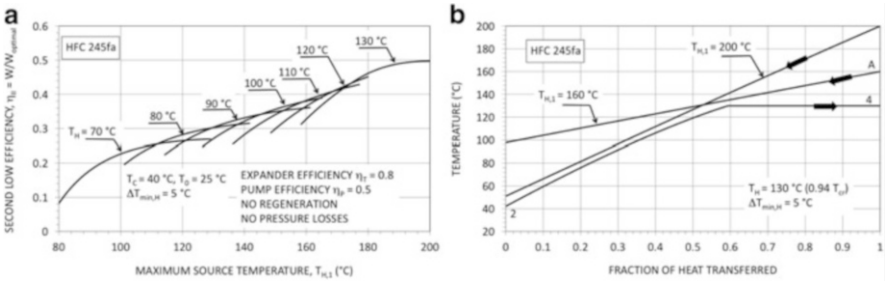

Fig. 3.19 (**a**) Efficiency of the second law for the thermodynamic cycle-heat source system, at varying maximum temperatures of the heat source $T_{H,1}$ and for different evaporation temperatures T_H for the working fluid (HFC 245fa). (**b**) Heat exchange diagrams for the thermodynamic cycle-heat source system

In general, from a strictly thermodynamic point of view, the cycle that exploits best a heat source of varying temperature (and that can be potentially cooled to nearly environmental temperatures) is the one which uses a working fluid of average molecular complexity, with a critical temperature close to the maximum temperature of the source.

3.2. Having selected a determinate thermodynamic cycle, the conversion efficiency of the heat introduced is fixed and so too is the law of heat introduction which, in the normal case of saturated cycles, has the trend shown in Fig. 3.18: a first part characterised by variable temperature (preheating of the liquid), followed by an isothermal part (evaporation of the liquid). Having fixed both T_H and T_C, the cycle can be used for various heat sources, each at a different maximum temperature $T_{H,1}$, characterised by different degrees of cooling and with distinct overall levels of energy quality (that is, different η_{II} efficiency).

Having fixed T_H and, usually, a $\Delta T_{min,H}$ in the recovery heat exchanger, the cooling of the source is unequivocally identified, as shown, for example, in Fig. 3.19b: the source at temperature $T_{H,1} = 160\ °C$ is cooled down to a temperature that is higher than that to which the source was cooled with temperature $T_{H,1} = 200\ °C$. Which of these thermodynamic cycle-source combinations will give the best result cannot be foreseen a priori, but must be determined, for different fluids and, for each of these fluids, for different temperature extremes of the cycle. One example of the results is given in Fig. 3.19a for the case of HFC 245fa.

Having set $T_H = 70\ °C$, for example, the heat source that is best exploited is that with temperature $T_{H,1} \approx 110\ °C$, with $\eta_{II} \approx 0.25$. The envelope of lines at the different evaporation temperatures of the working fluid gives best combinations between the cycles (saturated) and the heat sources for the specific working fluid under consideration (HFC 245fa). In the case we analysed, the maximum value of the second-law efficiency was obtained with a reduced evaporation temperature of around 0.94 ($T_H = 130\ °C$) and stands at about 0.5, for heat sources with $T_{H,1} \approx 190–200\ °C$.

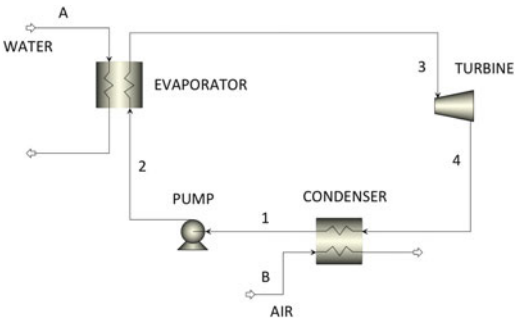

Fig. 3.20 Simplified drawing of the plant for Exercise 3.3

3.3. As discussed in Sect. 3.2, the choice of the most suitable working fluid for an organic fluid engine depends not only on its thermodynamic behaviour, but must also consider its thermal stability and its chemical compatibility with the materials used to make the plant.

In any case, the often inevitable decomposition should proceed relatively slowly, so that it does not substantially compromise the fluid characteristics and, thereby, deteriorate excessively the thermodynamic performance of the system. The effect of the working fluid decomposition on the thermodynamic efficiency of the engine is apparent firstly in a drop in useful power caused by the rise in condensation pressure, but the seriousness of the effects depends on the nature of the working fluid, its operating conditions and, clearly, the extent of the decomposition. Generally, when decomposition takes place, the products of the degradation have a simpler chemical structure than the initial working fluid, a lower molecular weight and single chemical bonds (for example, CH_4, CF_4).

With reference to a cycle with a hydrocarbon as working fluid (*n*-pentane, C_5H_{12}, critical temperature $T_{cr} = 196.55\,^{\circ}C$ and critical pressure $P_{cr} = 33.7$ bar), we analyse the variations in the useful power of the engine when, starting from the design conditions, part of the fluid degrades and impurities of various kinds begin to form. The calculations refer to "off-design" situations, in the simplified hypothesis of stationary conditions. For the sake of simplicity, the performance of turbine and pump are also considered constant as the maximum and minimum operating pressures vary.

The case considered regards a hypothetical geothermal source of hot water at high pressure. The plant scheme for reference is that in Fig. 3.20. Figure 3.21 shows the performance of the useful power as the evaporation pressure varies.

The maximum value of useful power per unit flow of hot water is reached in correspondence with an evaporation pressure P_E of about 12 bar and is equal to around 80 kJ/kg of hot water. Starting from the design conditions ($P_E = 12$ bar, $P_C = 1.393$ bar, mass flow of hot water $\dot{m}_A = 0.8895$ kg/s (for unitary mass flow of working fluid), air flow to the condenser $\dot{m}_B = 32.14$ kg/s, $(UA)_E = 29{,}050$ W/K, $(UA)_C = 27{,}082$ W/K) and assuming that the global coefficient of heat exchange U_E at the evaporator and the global coefficient of heat exchange U_C at the condenser do not change, we get the results in Fig. 3.22a, b.

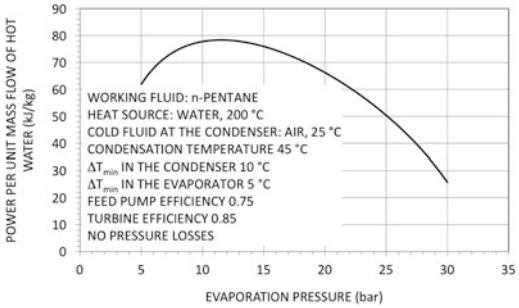

Fig. 3.21 Useful power as a function of the evaporation pressure

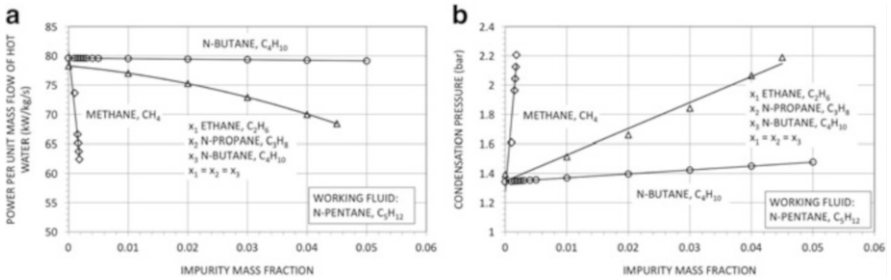

Fig. 3.22 Effect of the degree of impurity on (**a**) the useful power and on (**b**) the condensation pressure. The curves refer to the cases in which decomposition of the working fluid leads to the formation of just methane, just *n*-butane or a mixture of ethane, *n*-propane and *n*-butane

Figure 3.22a shows the eventual formation of very small quantities of methane are sufficient to compromise the plant operation: one mass fraction of methane of 0.002 reduces the useful power by 22 %, with a significant increase in the condensation pressure (from 1.393 to 2.2 bar; see Fig. 3.22b). By contrast, the formation of *n*-butane is less dramatic: one fraction of *n*-butane, equal to 0.05, reduces the useful power by less than 1 %, with a modest increase in the condensation pressure.

Where methane forms, though, its volatility makes it relatively easy to expel from the plant since it is particularly rich in the condenser, in the vapour phase (see Fig. 3.23). In this way, it is relatively simple to guarantee that the system operates properly. This would be completely different were the decomposition produces just *n*-butane: the vapour phase in the condenser is not particularly rich in it and its separation would, therefore, be rather difficult.

The conclusions in the example have a general qualitative validity, even though, the real effects of the decomposition of small quantities of fluid clearly depend on the type of fluid, the type of plant and the operating conditions (for example, super- or sub-atmospheric condensation pressures).

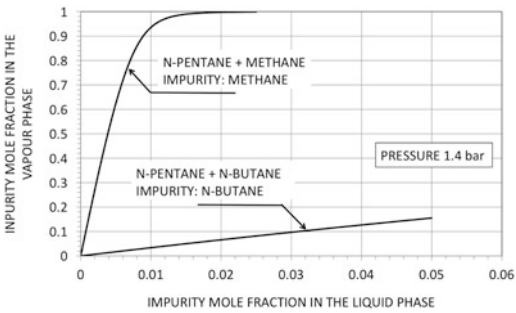

Fig. 3.23 Compositions of the vapour phase and the liquid phase for two mixtures of *n*-pentane

3.6 Some Examples of Applications of Organic Rankine Engines

There are numerous working fluids employed in Organic Rankine engines. They all have the potential to be thermodynamically adequate provided that they satisfy the requisites discussed in Sect. 3.2: adequate thermo-physical properties (thermodynamic and of heat exchange), appropriate thermal and chemical stability, compatibility with materials and substances present in the plant, safety of use and minimal environmental effects.

A list of the possible working fluids would not only not be exhaustive, but largely useless, given the number and range of families of organic products. In fact, every fluid should be considered and analysed specifically. For example, the toxicity depends greatly on the structure of the molecule and it can be misleading to generalise: the perfluorohexane (C_6F_{14}, of the family of perfluorocarbons), for instance, derived from hexane, substituting all the hydrogen atoms with fluorine atoms, used as a solvent and cooling fluid, is considered biologically inert and chemically very stable; the perfluoroisobutene ($(CF_3)_2C_2F_2$, also called PFIB, a fluorocarbon alkene, product of the pyrolysis of the polytetrafluoroethylene) is more toxic than phosgene ($OCCl_2$, one of the most infamous chemical weapons used during World War I). Table 3.5 reports the parameters of health hazard, inflammability and chemical reactivity for certain fluid families and for several compounds that are typical of every family.

In fact, organic fluid engines mainly use the following working fluids: hydrocarbons, perfluorocarbons, siloxanes, refrigerants, fluoro-alcohols (for example, 2,2,2-trifluoroethanol). Potential working fluids could be all those fluids used as heat exchange fluids in the industrial sector: siloxanes, fluids with biphenyl or chlorinated biphenyl as base compounds, the perfluorocarbons or the perfluoroethers.

As far as the effects on the environment are concerned, these are regulated by a host of complex and varied mechanisms, and typical parameters include the atmospheric lifetime, the ODP and the GWP (see Table 3.6). In this case, too, each compound should be characterised separately, but, as a general rule, short atmospheric lifetimes give low ODP and GWP. The molecules that do not contain

Table 3.5 Some data about health hazard, inflammability and chemical reactivity for certain families of organic fluids

Fluid	Health hazard[a]	Flammability[a]	Chemical reactivity[a]
Hydrocarbons			
Alkanes, alkenes, alkyne, cycloalkane, alkadienes	1	4	0
Toluene	2	3	0
Naphthalene	2	2	0
Biphenyl	1	1	0
Siloxanes			
MM[b]	1	4	0
D5[c]	1	2	0
Perfluorocarbons			
Perfluorohexane	0	0	0 - 1
Perfluorodecalin ($C_{10}F_{18}$)	0	0	0 - 1
Refrigerants			
Ammonia	3	1	0
HFC 134a[d]	1	0	1
Diethyl ether ($(C_2H_5)_2O$)	2	4	1
Miscellanea			
2,2,2-Trifluoroethanol (CF_3CH_2OH)	2	3	1
Tetrachloroethylene[e]	2	0	0
Pyridine (C_5H_5N)	3	3	0
Chlorobenzene	3	3	0

[a]According to NFPA 704: a standard of the National Fire Protection Association that characterises the health hazard, the flammability and the reactivity on a scale from 0 (no hazard, normal substance) to 4 (severe risk)
[b]Hexamethyldisiloxane: $(CH_3)_3SiOSi(CH_3)_3$
[c]Decamethylcyclopentasiloxane
[d]Hydrofluorocarbon (or refrigerant) 134a: 1,1,1,2-tetrafluoroethane
[e]It is a liquid widely used for "dry cleaning" of clothes

iodine, bromine or chlorine usually have null ODP, but are often characterised by long atmospheric lifetimes, which could be a problem.

In this section, we shall present and briefly discuss several important examples and typical applications of organic fluid Rankine engines.

A Low Temperature Solar Plant

It is still not completely certain that low temperature solar thermodynamic systems (without concentration) can produce competitively priced electricity. In any case, for this to happen, certain minimum requisites need to be met: highly efficient solar collectors and conversion systems (the heat engine), modest consumption by auxiliary engines and favourable climatic conditions.

Table 3.6 Data regarding the environmental effects of certain fluids and compound families

Fluid	Atmospheric lifetime	ODP[a]	GWP[b]
Hydrocarbons			
Alkanes, alkenes, alkyne, cycloalkane, alkadienes	10–15 years	0	3–4
Toluene	2–500 days		
Naphthalene			
Biphenyl			
Siloxanes			
Volatile methylsiloxanes (linear and cyclic)	10–30 days	0	
Perfluorocarbons			
linear and cyclic	3,000–4,000 years	0	9,000–1,000
Refrigerants			
ammonia	5–10 days	0	0
HFC 134a[c]	15 years	0	1,450
Diethyl ether ($(C_2H_5)_2O$)	10 years	0	4
Miscellanea			
2,2,2-Trifluoroethanol (CF_3CH_2OH)			
Tetrachloroethylene[e]	5–6 months	0	0
Pyridine (C_5H_5N)			
Chlorobenzene			

[a]The ozone depletion potential (ODP) relative to refrigerant 11
[b]Global warming potential (GWP) for given time horizon of 100 years and relative to CO_2
[c]Hydrofluorocarbon (or refrigerant) 134a: 1,1,1,2-tetrafluoroethane

Anyway, the solar plant of Borj Cedria (Tunisia) [23] and Fig. 3.24, was built in the 1980s with the very intention of evaluating the technical and economic feasibility of systems of this type. The power plant was financed by the European Community also with the aim of transferring solar technology and training Tunisian engineers. The company Belgonucleaire of Brussels was assigned responsibility for the project, its construction and management. The solar collectors (flat, single glass with a copper absorbing sheet and selective coating) were completely built in Tunisia, whilst the engine was designed and built in Italy. The principal data for the plant, under design conditions, are reassumed in Table 3.7.

The working fluid chosen for the engine was perchloroethylene (or tetrachloroethylene, $Cl_2C{=}CCl_2$), a nonflammable fluid, with a high critical temperature ($T_{cr} = 346.85\,°C$), a critical pressure $P_{cr} = 44.9$ bar and a boiling point of 121.25 °C. Its molecular weight is 165.83 and the parameter of molecular complexity $\sigma = 4.0$. The perchloroethylene, due to its excellent solvent properties, is still widely used in the dry-cleaning industry and in the metal cleaning.

When, as in this case, the temperature difference between the hot source and the cold well ($T_H - T_C$) (that is, the difference between the evaporation and the condensation temperatures) is moderate, the thermodynamic performance does not represent the key parameter in choosing the working fluid, since any fluid with a

Fig. 3.24 Photograph of the ORC plant of Borj Cedria (1982) (from author [1])

Table 3.7 Principal data for the solar plant of Borj Cedria, under design conditions[a] [23]

Total surface of collectors	750 m^2
Temperature of entry/exit for the collectors' manifolds	85.4/100 °C
Temperature of entry/exit for the motor	98.5/86.5 °C
Cooling water temperature	20 °C
Cooling water mass flow	6 kg/s
Daily performance of the collector field	0.33
Electricity per day (net)	80 kWh
Volume of the storage hot water	45 m^3
Daily consumption of the auxiliaries of the field	13.6 kWh
Daily consumption of auxiliaries of the engine	1.6 kWh
Rated output power (net)	12 kW

[a]Daily insolation 5 kWh/m^2 day, corresponding to a reference clear day, next to the equinox

sufficiently high critical temperature will give an acceptable performance. As far as the final performance is concerned, the efficiency of the individual components is more important: the turbine, the heat exchangers, the feed pump, the speed reducer and the alternator. These components all depend on the nature of the working fluid and on the power size (see Sect. 3.4). In the case described, the working fluid is chosen for the very intent of optimising both the thermodynamics and, especially, the performance of single components.

Figure 3.25 shows the plant layout, taken here as reference. Given the modest molecular complexity of the working fluid ($\sigma = 4.0$), the regenerator is not necessary. The evaporation temperature T_4 under design conditions is about 84 °C and that of condensation T_1 is 30 °C. The gross electrical power is 16 kW; the net power (under nominal conditions) is 12 kW. From the calculations carried out according to the scheme in Fig. 3.25, assuming an efficiency of the expander of 0.84 and an efficiency of the reducer–alternator group of 0.833, we get a gross efficiency of 9.5 %. The reduced evaporation pressure (around 0.34 bar) is responsible for a

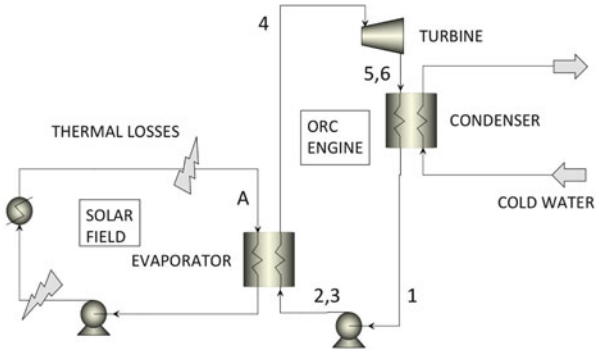

Fig. 3.25 Simplified scheme of the solar engine of Borj Cedria

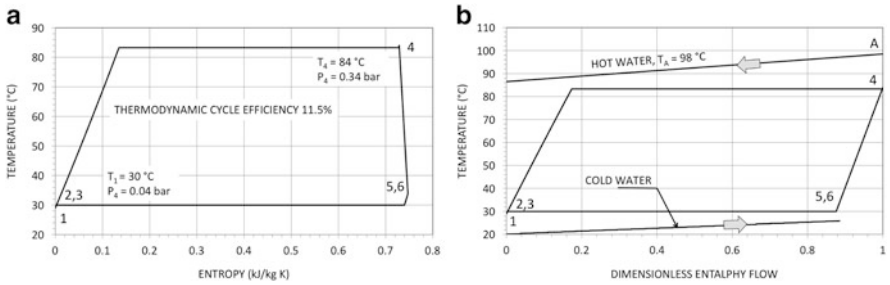

Fig. 3.26 Thermodynamic cycle of the solar engine of Borj Cedria. (**a**) Configuration of the thermodynamic cycle on the T–S plane. (**b**) Configuration of the cycle and heat exchange diagrams on the temperature–power plane

large volume flow at the turbine inlet and makes also it possible to eliminate the feed pump, substituted by the natural head of the liquid column, which feeds the evaporator, starting from the condenser located at an appropriate height (4–5 m).

The axial, mono-stage turbine, characterised by a large volume expansion ratio $\left(\dot{V}_{\text{in}}/\dot{V}_{\text{out}}\right)_S = 6.61$ and a modest specific work $(\Delta H)_S = 35.7$ kJ/kg, has a supersonic absolute vapour speed at the outlet of the fixed and rotating blades and subsonic relative speed at the rotor inlet and outlet. The rotation speed is 8,200 rpm. The maximum peripheral speed is about 180 m/s, with an average rotor diameter of 0.4 m and an average height of the rotor blade of about 1.8 cm.

In Fig. 3.26a the thermodynamic cycle is represented in the temperature–entropy plane and we see how the modest molecular complexity of the fluid and the modest difference between evaporation and condensation temperatures mean that the second-law efficiency of the cycle is very high ($\eta_{\text{II}} = 0.76$).

Figure 3.26b reveals the good match between the hot source and the cold source (the water for the condensation). The low maximum temperature of the heat source ($T_A = 98$ °C) gives a modest efficiency of global conversion and the ratio $\left(\dot{Q}_{\text{in}} + \dot{Q}_{\text{out}}\right)/\dot{W}$ is 19.6. There are high costs for the evaporator and condenser, to

which need to be added the costs of the solar field (also high, given the low efficiency of the collectors used).

The plant of Borj Cedria entered service at the end of June 1983 and operated correctly in both the solar and conversion sections. However, the cost of the energy generated proved to be very high, mainly due to the size of the heat exchangers and the extent of the solar field.

The Geothermal Binary Plants

The production of electricity from geothermal heat began thanks to the initiative of Piero Ginori Conti in 1904 at Larderello (Tuscany), with a geothermal steam engine and a dynamo of 10 kW. In 1913, the first commercial geothermal power plant was built (of 250 kW), again at Larderello, with the production and supply of electricity to the neighbouring towns.

In 1967, in the Soviet Union, one of the first binary power units was made at Paratunka, Kamchatka, with a heat source consisting of hot water at 80 °C, which, even today, represents one of the lowest temperatures ever exploited. Although the plant apparently functioned satisfactorily for many years, it was closed and dismantled towards the end of the 1970s—early 1980s due to leakage of the working fluid (the refrigerant R-12) [24]. Much earlier, in 1940, on the island of Ischia (Italy), a pilot binary geothermal plant was set up (see Sect. 3.1), but it never led to industrial development. An important example is the binary plant of 1.0 MWe at Nagqu, in North Tibet, at an average altitude of 4,500 m above sea level. It uses a geothermal source at 110 °C, with an air condenser, and became operative in 1993 [25, 26].

Today, about 11 % of the total 11,000 MW ca. installed power consists of binary plants: an organic fluid engine which, cooling the geothermal brine, produces electricity according to the usual scheme in Fig. 3.3, generally without a regenerator.

The binary systems are usually used when direct use of vapour is not possible and the temperature of the source, the geothermal brine, which is essentially liquid water with highly varying percentages of salts (NaCl, KCl, SiO_2), and gases (CO_2, H_2S) is not sufficient to make expansion of the geothermal fluid convenient (after the opportune flash). Shifting to binary cycle technology is considered convenient when the geothermal fluid consists mainly of water below the temperature of 150–180 °C. Looking to the future, if the forecasts and the technological endeavour now in progress for exploiting the engineered—or enhanced—geothermal systems (EGS) are correct and meet with success, then the interest in and potential of binary systems will certainly increase.

The binary system offers various advantages: it is generally more acceptable from an environmental point of view than any other geothermal power plant because the segregation of the geothermal fluid throughout the conversion process prevents the gas or other potentially polluting substances from being released into the environment; for sources with moderate temperatures (150–180 °C), they have better thermodynamic performances than the flash systems and can be used for the

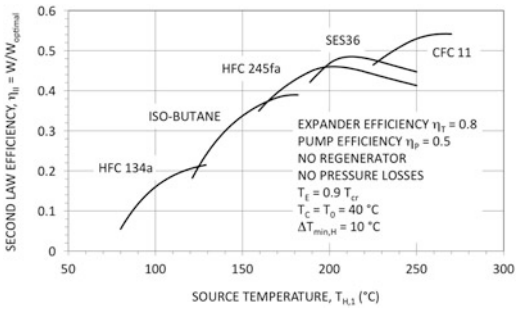

Fig. 3.27 Energy quality of the conversion as a function of the source temperature, for various working fluids

generation of electricity even with low temperature sources (90–100 °C); the binary systems reduce the problems connected with the scaling of fluids (the carbonate scale is prevented by installing downwell pumps, the silica scale is minimised, preventing the concentration growth caused by flashing). The cost of binary units is usually high but often compensated by the greater energy produced compared to flash systems.

The first European binary unit became operative in July 1992. The engine, with a gross electric power of 1.2 MW, was constructed by Italian companies under the EEC THERMIE programme and tested at Castelnuovo Val di Cecina, near to the geothermal power station of Larderello [27]. At the same time as the binary unit of Castelnuovo, there was that of "Travale 21" (in the district of Radicondoli, Italy): a binary power plant of 700 kWe.

In a binary plant, the choice of working fluid is a fundamental part of the project. Putting aside the characteristics of the heat exchange and the relative costs of the heat exchangers, at least two operative approaches are possible for the choice of working fluid: a fluid that will guarantee the highest conversion efficiency and a fluid that, once the power of the plant has been set, will permit the best design of the turbine. As we have already observed (see Sect. 3.5), if the heat source can be considered for the most part isothermal, optimisation of the thermodynamics is invariably favoured by a fluid with high critical temperature and a simple molecular structure. By contrast, when the heat source has a variable temperature, the maximum power is a combination of the engine fluid capacity to cool the source and, at the same time, the capacity of the thermodynamic cycle to best use the heat extracted from the source [28].

Figure 3.27 shows the performance of the second-law efficiency as a function of the maximum temperature of the geothermal water source for binary cycles using different working fluids. In Table 3.8, there are various thermodynamic properties of the fluids considered.

Each working fluid, according to its own critical temperature, exploits as best it can, the heat sources with maximum temperatures between the appropriate ranges. For instance, among the working fluids considered in the figure, HFC-134a would be advantageous from a strictly thermodynamic point of view for the exploitation of heat sources up to 120–130 °C, while the isobutane gives good thermodynamic

Table 3.8 Some data regarding working fluids used for the calculations in Fig. 3.27

Fluid	Critical temperature (°C)	Critical pressure (bar)	Boiling temperature (°C)	Acentric factor	Parameter of molecular complexity
HFC 134a	101.03	40.56	−26.07	0.3514	0.068080026
Isobutane	136.45	36.4	−11.72	0.183521	2.881631257
HFC 245fa[a]	154.05	36.4	15.3	0.375486	4.314297134
SES36[b]	177.55	28.49	35.64	0.3514	10.6252618
CFC 11[c]	198.05	44.08	23.82	0.189365	1.422963902

[a]Hydrofluorocarbon (or refrigerant) 245fa: 1,1,1,3,3-pentafluoropropane
[b]Solkatherm SSE36: an azeotropic mixture of refrigerant HFC 365mfc and a perfluoropolyether [29]
[c]Chlorofluorocarbon (or refrigerant) 11: trichlorofluoromethane

performances for sources from 120–130 °C up to 160 °C and so on. The refrigerant CFC-11, considered here just as an example, with a very high critical temperature, offers high second-law efficiency only if matched with sources with high maximum temperatures. Obviously, the various choices have a heavy influence on the turbine design. For example, if a source with maximum temperature of 100 °C is used with HFC-134a, in the examples in the figure, the condensation pressure will be 10.0 bar; if a source at 200 °C is used with HFC245fa, the evaporation pressure will be 2.42 bar. It follows, therefore, that a turbine at fixed revs would supply much greater power in the first case that in the second.

In general, a design project that aims at designing a low-pressure ORC means, at least for power ranges in the MW range, a turbine with a low number of revs can be used. By contrast, the solution of a high pressure ORC, using working fluids that operate with pressures close to critical pressures, requires, once the power is established, high-speed turbines (and feed pumps that consume more power).

In the case of the binary unit at Castelnuovo val di Cecina, the working fluid (the refrigerant CFC-11) was chosen to favour the design of the turbine. The CFC-11 was the only non-inflammable low-pressure fluid (with high critical temperature), and, in that period, the chlorofluorocarbons had not yet been phased out for environmental reasons.

One significant example of a geothermal plant with an ORC engine is the combined heat and power (CHP) plant at Altheim (Upper Austria). A geothermal district heating system had been in use since 1990 and the project of associating an ORC engine to the district heating was proposed to the European Commission in 1996.

The ORC turbogenerator and the well head, which are located near to the city in a densely populated area, required the use of a silent engine and a non-inflammable working fluid. One of the first to be completely built in Europe has a nominal power of 1,000 kWe. The ORC unit is cooled with water originating from a canal and the geothermal water is reinjected at a temperature of 70 °C into the deep geothermal Malm-aquifer [30]. The geothermal fluid is available at 106 °C and the high temperature downhole pump is installed at a depth of 250 m. The two

Table 3.9 Principal data of the Altheim power plant [31]

Source inlet temperature	106 °C
Source discharge temperature	70 °C
Source mass flow	81.7 kg/s
Electric power	1,000 kW
Generator speed	1,500 rpm
Cooling water inlet temperature	10 °C
Cooling water outlet temperature	18 °C
Cooling water mass flow	340 kg/s

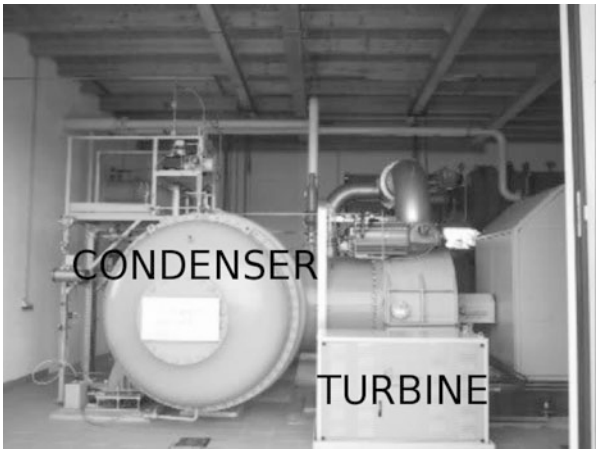

Fig. 3.28 An image of the geothermal ORC engine at Altheim (2000) (from author [32])

wells (one for production and the other for reinjection of the geothermal water) are about 2,300 and 2,170 m deep, respectively. The ORC engine was installed in spring–summer 2000 and the first tests began in September 2000. The working fluid chosen was perfluoro-*n*-pentane (perfluoro-*n*-pentane, C_5F_{12}).

In May 2005, perfluoro-*n*-pentane was completely substituted by a new fluid (known by its commercial name Solkatherm SSE36), with good heat exchange properties and low viscosity and characterised by excellent turbine fluid dynamics. Heat stability is ensured up to 225 °C. The basic thermodynamic properties of SSE36 are reported in [29]. Solkatherm SES 36, an azeotropic mixture that is 65 % hydrofluorocarbon, HFC265mfc (1,1,1,3,3-pentafluorobutane) and 35 % perfluoropolyether (Galdem HT55), was used for the first time as a working fluid in the plant at Altheim, to replace perfluoro-*n*-pentane. Data from the plant have been summarised in Table 3.9 and a photograph of the engine can be seen in Fig. 3.28.

The availability of the plant is very high, over 7,500 h/year, but priority is given to district heating and just the hot geothermal water not sent to the mains is available for producing electricity.

The choice, made during the engine design, to create a low pressure ORC (that is, opting for a working fluid with a condensation pressure not too dissimilar to the atmospheric pressure and an evaporation pressure far from the critical pressure) has led to a turbine of 1 MW, with just 1,500 rpm. Around half the total cost of the plant was due to the well for reinjecting the geothermal fluid.

The CHP Biomass Plants

By the term biomass, we mean all the material resulting from living organisms, excluding those which, although the result of biological processes, have remained trapped underground so long as to merit the term fossil. In current usage, the term biomass refers only to biomass of vegetable origin. The use of biomass for the production of heat and electricity, typically in CHP units, for instance, in the way described in Sect. 1.4, passes through thermochemical processes that make the energy content, of a chemical nature, of the biomass available. Generally speaking, there are three thermochemical processes of practical application for this transformation:

- Combustion, where (in the presence of a significant excess of oxygen) bringing the biomass to a high temperature (1,000 °C), the physical and chemical structures of the biomass itself are demolished. The completely oxidised products of the combustion are, essentially, carbon dioxide and water.
- Pyrolysis, during which the biomass structure is broken down thermally into simple compounds, without the addition of oxygen, because the heating takes place without contact with the atmosphere. The final products are fuel gas (composed of hydrogen, carbon oxide, hydrocarbons and inert gases) and charcoal.[25]
- The oxidative gasification, which follows a similar method to combustion, but with an added oxygen in sub-stoichiometric amount, in such a way as to obtain final gas products that are not completely oxidised, which can then be used as fuel gas.

The fuel gases from pyrolysis or gasification can be used in ICE (Otto cycle), gas turbines or Stirling engines. The gases produced by the combustion process can be used for the steam production (to be used in steam turbines) or, typically via a secondary circuit with diathermal oil, constituting the hot source for an ORC turbogenerator. In principle, any prime mover capable of converting external heat could be used: even Stirling engines (see Sect. 1.8) and gas turbines (see Sect. 1.7).

[25]Charcoal, obtained by pyrolysis of vegetable biomass, was the only secondary fuel used by pre-industrial societies. Coke, produced by the pyrolysis of coal, was used in England during the 1640s and replaced charcoal in iron smelting towards the middle of the 1700s, when its production costs had dropped sufficiently to make it competitive.

In the case of Stirling engines, there is a need (in order to guarantee good performance) to keep the volumes destined to heat exchange small compared to the swept volume of the cylinder and this means using very compact heat exchange matrices, with small hydraulic radii and high surface to volume ratio. Since the combustion gases of biomass in a furnace are often heavy with particles particulate, sometimes, in order to prevent fouling of the hot heat exchanger, it is necessary to resort to systems of gasification rather than direct combustion of the biomass. In any case, the power of commercial Stirling engines is generally limited to several dozen kW.

Often, large quantities of virgin biomass are available as residual product from pruning, from virgin wood working, from periodic forest clearing and maintenance or directly from the cultivation of particular vegetable species. Wood is often available as waste from production processes (sawmills, furniture industry).

As we have mentioned, in the typical layout for a biomass plant using an ORC engine, the biomass is burnt in a furnace, using well-tested techniques, in a process that can be considered safe, reliable, clean and efficient. A heat transfer oil is used as the intermediate medium for the heat exchange between the combustion products (at 900–1,000 °C) and the working fluid for the ORC engine (which must necessarily have relatively modest maximum operating temperatures; see Sect. 3.2). Use of the heat transfer oil permits the furnace to function at low pressures, eliminating the need for licensed operators (on various shifts) to be present, as requested for steam systems in many European countries. The Organic Rankine prime engine converts the heat into mechanical energy. If the thermodynamic engine is designed appropriately, the condensation heat can be recovered in order to produce hot water (for example between 80 °C and 120 °C), for use in district heating and other uses, including industrial use (wood drying, sawdust drying) or for absorption chiller.

The special characteristics of the ORC technology (the simple start-up and switch-off procedures, the silent operation of the engine, the limited maintenance needed and the good performance with partial loads, the furnace characteristics) are such that, when the plant is operating in CHP mode, it is not necessary for specially qualified personnel, with a specific knowledge of the production sector and energy conversion, to be present [45]. The electrical power of ORC units for commercial biomass are usually just one or two MW.

Figure 3.29 shows, on the temperature–power plane, the heat sources (gas products of the combustion and the heat transfer oil), the organic fluid cycle and the heating process of the condensation water for a typical configuration of an engine using biomass. In Fig. 3.29b, for the sake of clarity, the cooling line for the combustion products has been eliminated. The calculations were made with reference to a unit flow of gas products of combustion. The working fluid for the organic fluid cycle is MDM (octamethyltrisiloxane, see Table 3.3). The evaporation pressure was assumed to be 10 bar and that of condensation to be 0.15 bar. The isentropic efficiency of the turbine was set at 0.8, the mechanical efficiency at 0.96. The isentropic efficiency of the pumps was 0.75 and the mechanical efficiency was 0.95. For the sake of simplicity, the pressure losses were not taken into account. The pinch point temperature differences were assumed to be 25 °C in

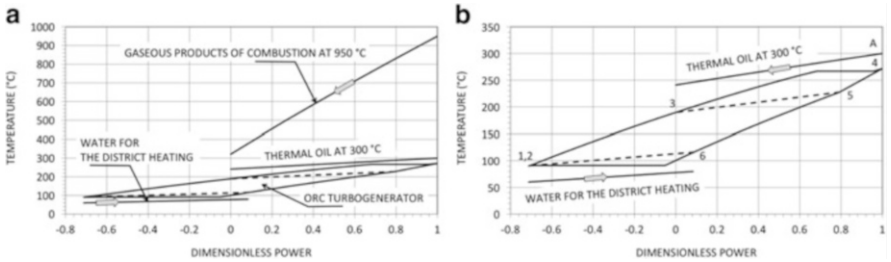

Fig. 3.29 Organic fluid engine for biomass. Configuration of the thermodynamic cycle and heat exchange diagrams in the temperature–power plane: (**a**) with the cooling line of the combustion products, which constitutes the heat source at high temperature, and (**b**) with just heat transfer oil, which decouples the organic fluid engine from the furnace. The working fluid for the engine is MDM (octamethyltrisiloxane)

the regenerator of the thermodynamic cycle and 15 °C for the condenser and for the secondary exchanger thermal oil-MDM.

The efficiency of the organic fluid cycle is 0.20 (considered as the ratio between the useful mechanical power and the thermal power made available by the diathermal oil). Ignoring the irreversibility of combustion (see Appendix B.1), the heat exchange exergy loss between gas products of the combustion and thermal oil is about 37 % of the exergy made available by the cooling up to $T_0 = 60$ °C of the combustion products. The exergy loss of the heat exchange oil-MDM is responsible for 0.7 % of the total losses, that of condensation for 7 %. The high exergy loss of the primary exchanger hot gas–thermal oil is due to the great difference in average logarithmic temperature between the two flows (279 °C). The thermal power regenerated per unit of useful mechanical power is about 3.5 (with a corresponding exergy loss of around 5.5 %).

Reducing the significant thermodynamic loss between gas products of the combustion and thermal oil is not easy and could, in principle, require the creation of systems with binary cycles (see, for example [33]), but careful consideration must be given to the increased plant costs that would be incurred in order to improve efficiencies.

One important example of an ORC biomass plant is the CHP plant of Lienz (East Tyrol, Austria) [34], which has been operative since 2001 and was built with financial funding from the European Commission within the fifth Framework Programme. The overall system consists of two biomass combustion plants: a hot water boiler, with nominal thermal power of 7,000 kW and a thermal oil boiler with nominal capacity of 6,000 kW.

The fuel used is biomass (wood chips, sawdust and bark, with a humidity content between 40 % and 55 %), originating from the nearby forests and the local wood industries. The electrical efficiency of the ORC unit (from 1,000 kWe, with hot water temperature at the condenser of 85 °C) is 18 %, which drops to 16–17 % and to 14 %, respectively, with a power of 50 % and 30 % of the nominal value: this testifies to the engine's great elasticity. Taking into consideration the plant

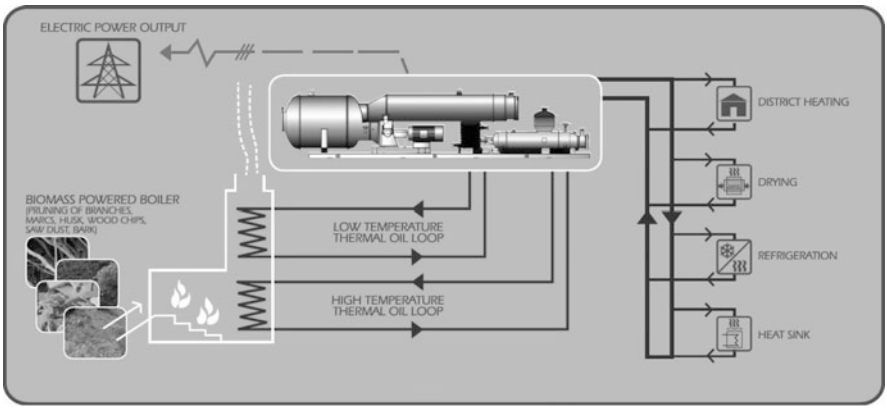

Fig. 3.30 Scheme for a biomass system with cogenerative organic fluid engine (with permission of Turboden srl)

Fig. 3.31 Photograph of the biomass plant with organic fluid Rankine engine at Fiera di Primiero in Trentino-Alto Adige (Italy). The engine installed (in cogenerative mode) has an electrical power of 1 MW (with permission of Turboden srl)

auxiliary systems, the (net) electrical efficiency drops to 15 % at the nominal power. In the winter season, the organic fluid thermal engine even works at 110–120 % of the nominal electrical load without prejudicing performance. At a nominal electrical load, the thermal power recovered at the condenser of the ORC unit is 4,440 kW. The biomass furnace is fitted with a preheater of the combustion air and an economiser for the thermal oil. The organic fluid engine works at full load for about 6,000 h/year.

Figure 3.30 represents a typical plant scheme for a CHP system with an organic fluid engine, Fig. 3.31 shows an ORC biomass plant in Trentino-Alto Adige (Italy) and Fig. 3.32 represents part of an organic fluid engine: the evaporator and the regenerator–condenser are shown.

Fig. 3.32 The biomass organic fluid Rankine engine at Varna, in Val d'Isarco (Italy). Cogenerative biomass engine with electrical power of 1 MW (with permission of Turboden srl)

Recovery of Waste Heat From Industrial Processes

The production cycles in many industrial sectors are often characterised by large quantities of waste thermal energy available in the process fluids. Typically gaseous fluids with highly variable mass flows and temperatures. After reuse of the fraction of thermal energy necessary for optimising the technological process, the remaining heat can be used to produce electricity (provided there are the necessary technical and economic conditions).

There are numerous sectors of potential interest: the cement industry (which typically provides heat from the combustion gases of the furnaces—downstream from the preheating of the raw materials—with temperatures of around 250–400 °C and from the cooling air for the "clinker", at temperatures lower than 300 °C), the steel-working industry (where the waste thermal energy is available from the process fumes and from fumes of the steel plants or foundries, often rich in powders), the glass industry (with availability of gases from the fusion of the glass at high temperatures of 400–600 °C), the petrochemical sector, ceramic production, heat recovery from the exhaust gases of diesel engines, etc.

In general, ORC technology enables heat recovery from any industrial process where waste thermal power is available in sufficient quantities to guarantee the design of engines with adequate efficiency at a reasonable cost.

With reference to strictly thermodynamic aspects, as illustrated in Sect. 3.5, in the case of a waste heat recovery system (WHES), with a heat source at variable temperature, the useful mechanical power per unit of available thermal power, the global efficiency η, is:

$$\eta = \frac{\dot{W}}{\dot{m}_{\mathrm{H}}\left(H_{\mathrm{H},1} - H_{\mathrm{H},0}\right)} = \frac{\dot{W}}{\dot{m}_{\mathrm{H}}\left(H_{\mathrm{H},1} - H_{\mathrm{H},2}\right)} \frac{H_{\mathrm{H},1} - H_{\mathrm{H},2}}{H_{\mathrm{H},1} - H_{\mathrm{H},0}} = \eta_{\mathrm{C}} \times C_{\mathrm{TU}} \quad (3.12)$$

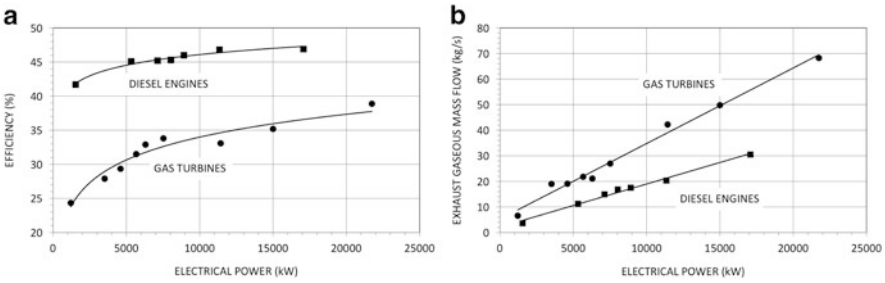

Fig. 3.33 A comparison between the characteristics of diesel engines and commercial gas turbine engines. (**a**) Efficiency as a function of electrical power. (**b**) Exhaust mass flow rate as a function of electrical power

with η_C representing the efficiency of the thermodynamic cycle and C_{TU} the coefficient of thermal utilisation. The global efficiency is, therefore, the result of two contrasting thermodynamic characteristics: the capacity to convert a high percentage of recovered heat into work (that is, a large η_C, which requires a high evaporation temperature T_H) together with a significant cooling of the heat source (which, inevitably, increases if T_H diminishes; see Sect. 3.5).

Having chosen the working fluid for the thermodynamic cycle, the consequences are that there is an optimal evaporation pressure and that, generally, the best working fluids have (1) a molecular complexity that is not too high and (2) critical maximum temperature close to the heat source (see Exercises 3.1 and 3.2). Ensured the thermal stability and taking into account the safety aspects of the fluid and its costs.

As an example of the specific application of ORC technology to heat recovery, we consider the case of recovering heat from the exhaust gases of a diesel engine.

The efficiencies as a function of the electrical power for some typical diesel engines and for gas turbines of similar power, in gen-set configurations, are reported in Fig. 3.33a. The electric efficiency of the diesel engines is always greater than the efficiency of the gas turbines of the same power: a difference of about 17 points per cent at 1.5 MW (about 25 % for the turbo gas and about 42 % for the diesel engine) and +11 points at 15 MW. The effect of the power size on the conversion efficiency is more pronounced in the gas turbines than in the diesel engines. For example, from 1.5 to 15 MW (a tenfold rise in power), the efficiencies of the diesel engines increase by a factor equal to 1.12 (from about 42 % to about 47 %) and the efficiencies of the gas turbines rise by a factor of 1.44 (from 25 % to 46 %). This is also a direct consequence of the difficulty in designing efficient, small and fast rotating turbomachines.

Figure 3.33b represents the mass flow of the exhaust gases as a function of the electric power for several diesel engines and gas turbines. At 15 MW, for example, the exhaust mass flow is about 27 kg/s for the diesel engine and 50 kg/s for a gas turbine of the same power: a value which is almost double. For the gas turbines considered in Fig. 3.33b, the mass flow rate per unit kW is 0.003 kg/s/kW: about 1.8 higher than that typical of diesel engines of similar power.

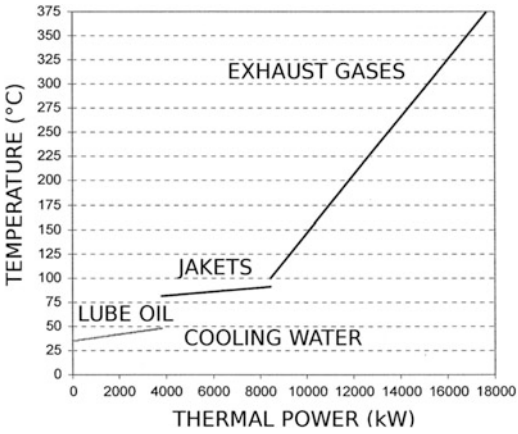

Fig. 3.34 Temperature and discharged thermal power for a typical heavy-duty diesel engine of 17 MW [35]

The smaller mass flows and the lower temperatures of the exhaust gases that are characteristic of the diesel engines (300–350 °C) compared with the gas turbines of similar power (400–500 °C) make the heat recovery more difficult.

Unlike gas turbines, in which the unconverted fraction of the chemical energy of the fuel is prevalently in the exhaust gases, in diesel engines it is discharged by (1) the exhaust gases (about 30 % of the LHV of the fuel), (2) the water cooling system of the jackets (and intercooler) (about 13 %) and (3) lubrication oil (about 10 %) [35].

Usually, (1) the exhaust gases have a maximum temperature of 350–400 °C and are at ambient pressure, (2) the water from the cooling of the jackets is available at about 90–100 °C, (3) the heat from the cooling of the lubrication oil is generally available at a temperature of about 50 °C: too low for an economic direct conversion into electrical energy. However, the heat at a lower temperature could be recovered in the heat exchangers of the plant to improve the overall energy balance.

With reference to a typical heavy-duty diesel engine of 17 MW, Fig. 3.34 reports the temperatures and the recoverable thermal powers from the exhaust gases and from the cooling water. The exhaust gases are available from $T_A = 375$ °C and are potentially cooled to 100 °C. The heat in the exhaust gases is about one half of the overall heat available and their relatively high temperature requires a recovery thermodynamic cycle operating with a working fluid of a high critical temperature.

In Fig. 3.35, we see a possible plant layout for recovering heat from a diesel engine. The working fluid of the Rankine cycle organic engine must have a high critical temperature and, as in the calculation example, toluene has been considered: $T_{cr} = 318.6$ °C, $P_{cr} = 41.08$ bar, $\sigma = 11.19$.

Several characteristics of the diesel engine used as reference are reported in Table 3.10. The composition assumed for the engine exhaust gases is the following (in molar fractions): 74.6 % nitrogen, 11.7 % oxygen, 6.7 % water, 5.9 % carbon dioxide and 1.1 % argon.

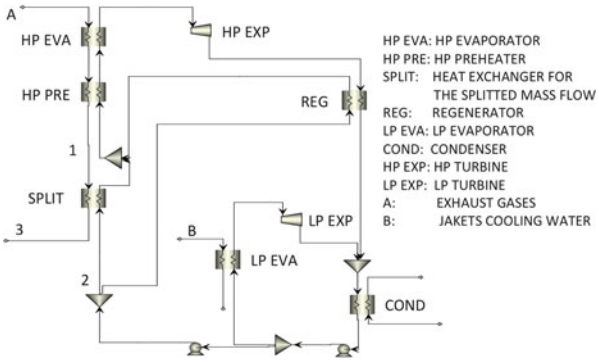

Fig. 3.35 Layout of a system for recovering heat from exhaust gases and from cooling water in a diesel engine [35]

Table 3.10 Several characteristics of the heavy-duty diesel engine considered for the calculations [35]

Electrical power	17,076 kW
Electrical efficiency	46.9 %
Temperature of the exhaust gases	374 °C
Exhaust gaseous mass flow	30.5 kg/s
Temperature of the jackets cooling water	80–91 °C
Cooling water mass flow	110.9 kg/s
Number of cylinders	18
Bore	460 mm
Engine speed	750 rpm

The cooling water in the engine, available at $T_B = 91$ °C, is cooled down to 81 °C on the low-pressure evaporator. The vapour of toluene (at 0.336 bar), expanding in the low-pressure turbine, produces 330 kW electric. The high pressure turbine (at 8.062 bar) generates 1,762 kW electric and the heat for preheating and the high pressure evaporation derives from the cooling of the exhaust gases of the engine from the temperature $T_A = 374$ °C down to $T_1 = 161$ °C, with direct heat exchange between the working fluid of the organic fluid engine and the gases of the diesel engine. In point 2, the flow of toluene is subdivided into two: one fraction (65 % of the flow on the high pressure turbine) goes over the regenerator and the remaining fraction, via the recovery exchanger denominated "split" in Fig. 3.35, further cools the exhaust gases of the diesel engine to the temperature $T_3 = 127$ °C. This introduces two thermodynamic advantages: a reduction in the irreversibilities of the heat exchange in the regenerator (see Fig. 3.10) and a greater cooling of the engine gases, which, otherwise, on account of the necessary presence of the regenerator, would be discharged into the environment at temperature T_1.

The net electrical power of the organic fluid engine is 2,072 kW, with a global efficiency of the combined system of diesel engine and organic fluid engine of 52.59 % (against a value of 46.9 % for just the diesel engine).

As far as the turbines are concerned, the high pressure one, with an isentropic enthalpy drop of about 170 kJ/kg, is rather loaded and, generally speaking, will require three axial stages; the low pressure one (with an isentropic work of about 44 kJ/kg) could be made with just a single axial stage.

Naturally, besides the purely thermodynamic analysis, a more detailed analysis of the return on investment would be needed to assess the economic viability of the plant (the cost of the heat exchangers, for example, is generally very high). However, the results of the above analysis give an idea of what can be expected from this kind of application, with a primary recovery of the exhaust gases and, possibly, the simultaneous recovery of cooling water from the engine.

In order to determine characteristics and costs of the ORC unit to be built, it is necessary to have accurate data from measurements of the temperature, the flows and about the nature and composition of the thermal sources. Apart from the nature of the fluid to which the thermal recovery is to be applied, the flows and temperatures must be noted in detail, including the variations they may undergo during the production process. The system available for the condensation (air or water) is also very important. In general, the size and costing of the heat recuperator exchanger require detailed data on the nature of the heat source (liquid or gas), such as its chemical composition, any polluting content (aggressive powders or chemical compounds) and the need to guarantee fixed temperature intervals (for instance, for the filtration or to prevent the appearance of incrustation and corrosion). On the basis of these characteristics, it is possible to establish the type of material needed, the exchange surfaces, the geometry and, consequently, the cost. Finally, it is important to determine the impact in terms of layout that the plant could have on the production process: modifying the existing lines could be especially costly, in particular, whenever there are problems linked to space availability and plant access.

As a general guideline, to be feasible, plant costs should not be greater than 3,000 euro/kW. The cost of electricity (difficult to predict in future years), the working time (in h/year) and expectations for the return on investment are all determining factors in the final choice.

The examples and the applications that we have presented and discussed (significative, although certainly not exhaustive) show how the choice of working fluid for each application is actually influenced by many factors: turbine enthalpy drops and flow rates, costs (of the fluid and the heat exchangers[26]), pressure levels, environmental compatibility, type of heat source, inflammability, type of cooling system, type of control system and supervision of the plant. In conclusion, the ideal fluid varies from case to case. Although, in principle, the organic fluid cycles adapt to every heat source (with maximum temperatures varying from 90–100 °C up to 300–400 °C) and to every level of power. Further research and development is, and always will be, needed to improve the heat exchangers, the expanders and in the study of new working fluids, possibly even multicomponent.

[26]The dimensions of the heat exchangers depend on the thermal power but also on the transport properties of the fluids, which directly influence the heat exchange coefficients.

3.7 Multicomponent Working Fluids for Organic Rankine Cycles

In principle, the working fluid used in an ORC could also be a mixture of two or more components: an azeotropic mix (for instance, the Solkatherm SES36; see Sect. 3.6) or a non-azeotropic mix. The non-azeotropic mixtures (see Exercises 2.2 and 2.1), once the pressure is set, are characterised by a difference, which may be more or less marked, depending on the fluids that compose the mixture and on the composition, between the dew and the bubble temperatures: the so-called temperature glide. That is, for the non-azeotropic mixtures, the liquid–vapour phase at constant pressure is not isothermal.

In practice, the presence of a temperature glide in evaporation could be useful from the thermodynamic point of view in those cases where the heat source is not intrinsically isothermal (as a possible alternative to the supercritical cycles), for example, in the heat recovery of flue gases exhausted by gas turbines or diesel and gas engines, or in the case of geothermal fluids and liquid-cooled solar collectors (see Sect. 3.5). If air is used for the condensation (with its modest heat capacity), the non-isothermal condensation may still be useful in reducing the flow of air necessary [36]. In the case of CHP systems for district heating, the condensation heat must be transferred to a liquid water loop, often characterised by a significant temperature difference between the delivery and the return from the heat consumers, and, in this case too, the use of heat engines with non-azeotropic mixtures could be thermodynamically appropriate.

By mixing several fluids, the critical point, too, varies continually (even in a non-linear way; see Exercise 2.2) and this characteristic may prove useful in creating thermodynamic cycles (see Sect. 4).

There are numerous fluid mixtures that could potentially be used (mixtures of hydrocarbons, fluorocarbons, polysiloxanes [36, 37] and, even, mixtures of non-miscible fluids [38]). Obviously, the criteria behind the choice of the best working fluid are still those briefly described in Sect. 3.2 and the aspects of interaction between the thermodynamics and the various components that make up the engine are still fundamentally those discussed in Sects. 3.3 and 3.4.

To highlight the peculiar characteristics of the non-azeotropic mixtures with a high temperature glide, in this section we consider, as a typical example, various cycles with ammonia–water mixtures of differing composition as the working fluid, assuming that the heat source is variable in temperature.

With reference to the scheme in Fig. 3.3 (a typical plant layout for an organic fluid engine), but without the regenerator, the performance of thermodynamic cycles has been calculated, considering ammonia–water mixtures of different molar composition as the working fluid. The heat source is water at 200 °C and the fluid used for condensation is air at 25 °C. For simplicity's sake, the water source is assumed coolable without any hindrance, down to room temperature. For the turbines and feed pumps, isentropic efficiencies of 0.75 are assumed and an efficiency of 0.95 to take into account the mechanical and electrical losses.

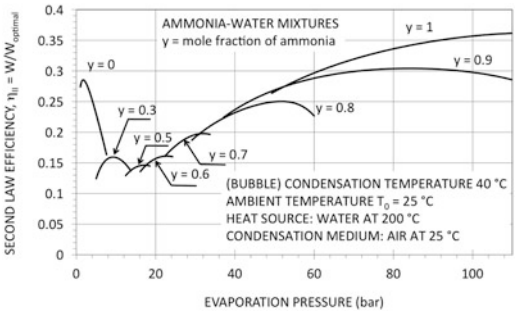

Fig. 3.36 Second law efficiencies for cycles with ammonia–water mixtures, with different molar compositions, as a function of the evaporation pressure

Again, for the sake of simplicity, pressure losses have not been taken into account. No limit was set a priori on the final temperature of the air necessary for the condensation. The logarithmic mean temperature differences on the exchangers have always been assumed, whenever it was possible to fix them beforehand, equal to 10 °C: a limit value that may be at the limit of technological practicability, but chosen in order to emphasise the importance of the heat exchangers, which, in the case of multicomponent fluids, are fundamental in order to highlight their thermodynamic characteristics.

Figure 3.36 shows the second-law efficiency η_{II} (for definition, see Exercise 1.2) for the various cases considered and for the cycles with pure fluids, water ($y = 0$) and ammonia ($y = 1$) as reference. The environment temperature T_0 has been taken as 25 °C for the purpose of calculations and the condensation temperature (that is, the condensation bubble temperature, in the case of mixtures) has been considered equal to 40 °C. The equation of state used to describe the thermodynamic properties of the mixtures is (2.5) with the mixing rules (2.30) and $\delta_{12} = -0.2589$.

The pure fluids (water and ammonia) tend to have higher η_{II} values than in the case of mixtures. This is a consequence of the different distribution of the entropic losses: on the machines, with regard to the heat source and the air used for the condensation and with regard to the environment taken as reference (at temperature T_0). The optimal η_{II} increases with the molar fraction y of ammonia and, at the same time, the optimal evaporation pressure rises.

Figure 3.37 shows just the losses in thermodynamic efficiency $\Delta\eta_{II}$ in the heat exchangers (heater and evaporator and condenser) at the maximum η_{II} for the mixtures considered. The mixture with molar composition equal to 0.7 in ammonia is that with the least entropic losses over the heat exchangers. The cycle with water vapour ($y = 0$) has, of all the cases considered, the highest loss in preheating and evaporation ($\Delta\eta_{II} = 0.035$) and the lowest loss in condensation ($\Delta\eta_{II} = 0.014$). For the ammonia–water mix with molar composition of 0.7, the losses over the heater and in condensation are 0.014 and 0.016, respectively.

The mixtures under consideration were shown to have an advantage in their single thermodynamic interaction with the sources. In particular, in the example discussed here, the mixture with $y = 0.7$ was the best. This has a direct consequence on the air flows requested by the condensation.

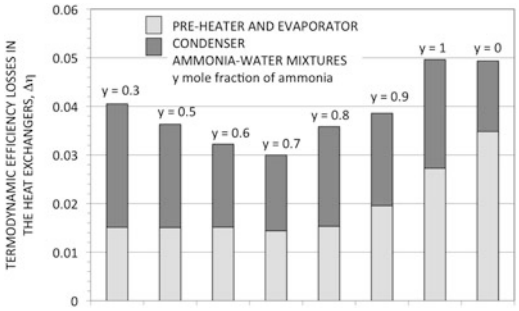

Fig. 3.37 Thermodynamic efficiency losses for heating and evaporation and for condensation in cycles with ammonia–water mixtures and with different molar compositions. Each case refers to the conditions of maximum second-law efficiency

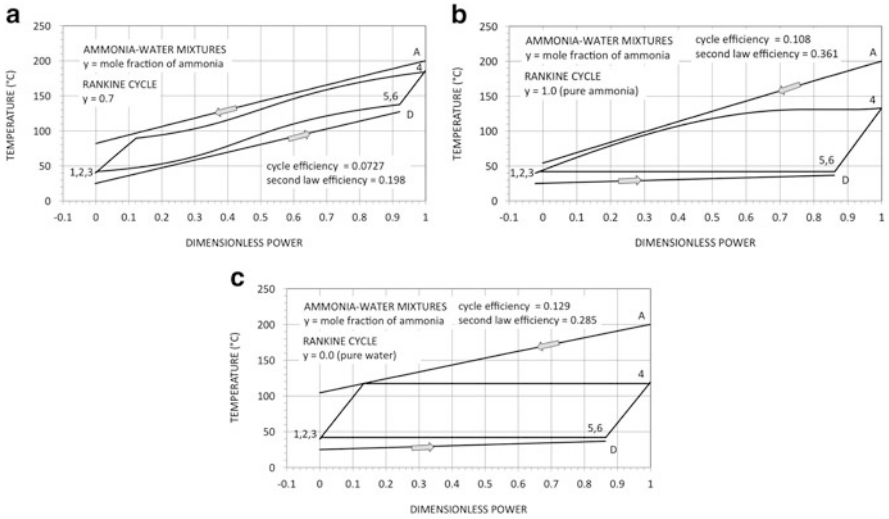

Fig. 3.38 Cycle configurations and heat exchange diagrams on the temperature–power plane, for different working fluids. The plant scheme for the cycle is that in Fig. 3.3, without regenerator. (**a**) Ammonia–water mixture. (**b**) Ammonia. (**c**) Water

Figure 3.38 represents, on the temperature–power plane, the thermodynamic cycles (each at the corresponding evaporation pressure of optimal second law efficiency) for the case of a working fluid consisting of an ammonia–water mixture, with molar fraction $y = 0.7$ in ammonia (Fig. 3.38a), for pure ammonia (Fig. 3.38b) and for water (Fig. 3.38c).

The heat exchange diagrams on the heater and the condenser justify the values of the various $\Delta\eta_{II}$ terms in Fig. 3.37. The air flows necessary for the condensation, per unit of gross useful power, are 0.119 kg s^{-1}/kW for the case of the ammonia–water

mix with $y = 0.7$, 0.688 kg s^{-1}/kW for pure ammonia and 0.565 kg s^{-1}/kW for water.

The air flow necessary for the condensation, gross useful power being constant, is, in the case of the steam cycle, around five times greater than that necessary for the condensation of the ammonia–water mixture; while the air flow necessary for the pure ammonia cycle is about six times greater. The power needed for pumping the air grows in direct proportion to the flow and, consequently, the net useful power diminishes. This could constitute enough of an advantage to justify the use of the mixture as the working fluid.

By contrast, though, the high temperature glide in condensation that is characteristic of the ammonia–water mixture in question is responsible, in the case of mixture with molar fraction $y = 0.7$, of the high final temperature of the air ($T_D = 127.3$ °C, in Fig. 3.38a). Above and beyond any problems this might give the plant, it leads to a significant thermodynamic loss (the exergy of the hot air is not to be considered a useful thermodynamic effect, unless the plant is cogenerative).

In the case of the three cycles, the condensation pressures are very different from each other: 0.0698 bar in the case of steam, 16.33 bar for pure ammonia and 10.32 bar for the ammonia–water mix with $y = 0.7$. The outcome of this is discussed in Sect. 3.4.

Appropriate modifications to the plant layout can raise the thermodynamic efficiency of the cycle in Fig 3.38a, with a mixture as the working fluid. Introducing a regenerator at the outlet of the turbine (according to the usual layout in Fig. 3.3) certainly increases the cycle efficiency and, in the case of the cycle in Fig. 3.38a, reduces the temperature T_D of the air at the condenser outlet. Introducing a regenerator also results in a minor cooling of the heat source, with a reduction of the useful power, and, ultimately, it is not sure that the second law efficiency will improve significantly. An alternative is to split the flow at the outlet of the feed pump, according to the scheme in Fig. 3.39a (and in Fig. 3.35, for a similar case of heat recovery at high temperature), seeking a good thermodynamic compromise between a sufficiently low temperature T_C and a reasonably high cycle efficiency (see Sect. 3.5).

Other configurations, partly repeating the plant layouts for absorption cooling cycles, foresee a separation of the steam phase, which is rich in ammonia, before the expansion, in such a way as to get a sufficiently low expansion temperature T_5. A typical example is the Maloney and Robertson cycle [39,40], of Fig. 3.39b (which also shows a superheater that is not present in any of the examples carried out here).

For example, in the Kalina cycle, in the version of Fig. 3.39c [40], which represents a more sophisticated version of the Maloney–Robinson cycle, the mixture flow available at the maximum pressure P_3 and at the evaporator composition $y_{1'}$ is further cooled by a second condenser, down to the temperature $T_{1'}$, before being sent to the heater and the boiler. Furthermore, there is a split in the flow after the low pressure compression.

The results of the second-law efficiency (for ammonia–water mixture with a base composition $y = 0.7$) are given in Fig. 3.39d. For comparison, the figure also shows

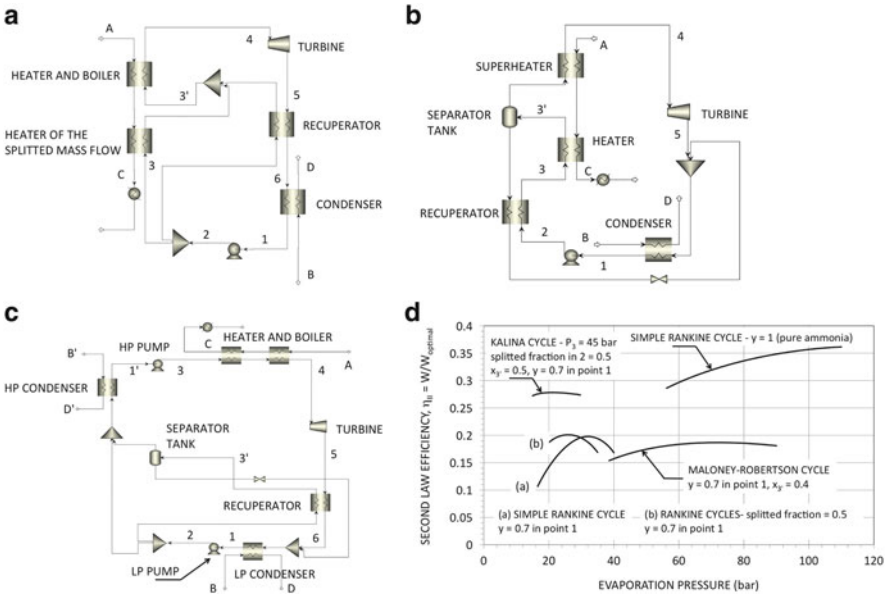

Fig. 3.39 Different plant configurations for cycles with ammonia–water mixtures. (**a**) Rankine cycle with flow split after the feed pump. A fraction of the high pressure flow passes across a regenerator (recuperator) and the rest cools the heat source. (**b**) Maloney and Robertson cycle. (**c**) A simple version of the Kalina cycle. (**d**) Results of second-law efficiency for cycles with ammonia–water as working fluid. In the case of the Kalina cycle, the abscissa represents pressure P_2. All the cases considered refer to saturated cycles, with a (bubble) condensation temperature of 40 °C, ambient temperature of 25 °C, heat source water at 200 °C and condensation air available at 25 °C

the curves relative to the Rankine cycle with $y = 1.0$ (pure ammonia). All the cases considered refer to saturated cycles. In the case of the Kalina cycle, the pressure in abscissa of Fig. 3.39d represents the pressure at point 2 in Fig. 3.39c.

Figure 3.40 gives the cycle configurations on the temperature-exchanged power plane, corresponding to the conditions of maximum second-law efficiency, with the corresponding values of the cycle efficiency and the second law.

Aside from the thermodynamic performance, when using multi-fluid mixtures, it should be noted that the coefficients of heat exchange are lower than those of the corresponding pure fluids [41–43]. In the specific case of ammonia–water mixtures, their use would normally be incompatible with carbon steels and aluminium for the problem of corrosion, so stainless steels or titanium are required instead [44].

The analysis above shows how the multi-component mixtures with a high glide temperature, among which the ammonia–water mixtures represent merely one example, are characterised by special thermodynamic properties, making it neither simple nor straightforward to choose which mixture to use or the plant set-up to adopt.

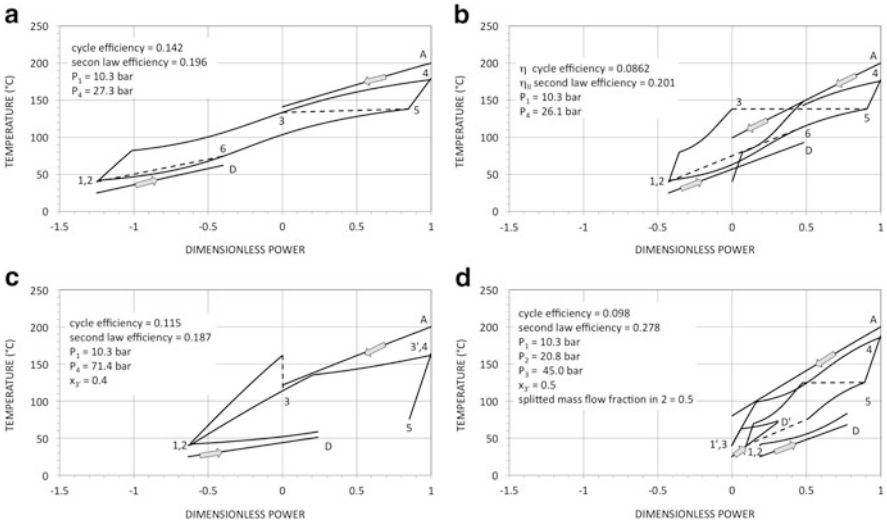

Fig. 3.40 Different configurations of the thermodynamic cycle on the temperature–power plane. (**a**) Rankine cycle with regenerator (plant scheme in Fig. 3.3). (**b**) Rankine cycle with regenerator and flow split after the feed pump (plant scheme in Fig. 3.39a). (**c**) Maloney and Robertson cycle (Fig. 3.39b). (**d**) A version of the Kalina cycle (Fig. 3.39c). All cases considered refer to saturated cycles, with a (bubble) condensation temperature of 40 °C, ambient temperature of 25 °C, heat source water at 200 °C and condensation air available at 25 °C

Certain plant configurations proposed are highly complex and all require sophisticated heat exchangers if they wish to make the best use of the specific thermodynamic properties of the non-azeotropic multi-component mixtures. Apart from the strictly thermodynamic considerations, the choice must also consider aspects directly linked to the plant and the machinery (operating pressures, fluid used for condensation, pump power).

References

1. Gaia M (2012) Thirty years of organic Rankine cycle development. In: First international seminar on ORC power systems, Delft TU-Technical University, The Netherlands, September 22–23 (Key-note presentation)
2. Rankine WJM (1859) A manual of the steam engine and other prime movers. Richard Griffin, London (Publishers to the University of Glasgow)
3. Anonymous (1827) Register of the arts and sciences – volume the fourth. A correct account of several hundred of the most important and interesting inventions, discoveries, and processes illustrated with about two hundred engravings. B. Steill, London
4. Stuard R (1829) Historical and descriptive anecdotes of steam-engines, and of their inventors and improvers, vol 1. Wightman and Cramp, London
5. Galloway E, Herbert L (1836) History and progress of the steam engine; with a practical investigation of its structure and application. To which is added, an extensive Appendix,

containing minute descriptions of all the various improved boilers; the constituent parts of steam engines; the machinery used in steam navigation; the new plans for steam carriages; and a variety of engines for the application of other motive powers, with an experimental dissertation on the nature and properties of steam and other elastic vapours; the strength and weight of materials, etc. Thomas Kelly, London
6. Ewing JA (1926) The steam-engine and other heat-engines, 4th edn. The University Press, Cambridge
7. Spencer LC (1989) A comprehensive review of small solar-powered heat engines: part I. A history of solar-powered devices up to 1950. Sol Energ 43(4):191–196
8. d'Amelio L (1935) The use of vapours with high molecular weight in small turbines. INAG – Industria Napoletana Arti Grafiche, Napoli (in Italian)
9. Spencer LC (1989) A comprehensive review of small solar-powered heat engines: part II. Research since 1950 – "conventional" engines up to 100 kW. Sol Energ 43(4):197–210
10. Duffie JA, Beckman WA (1991) Solar engineering of thermal processes, 2nd edn. Wiley, New York
11. El-Wakil MM (2002) Powerplant technology. McGraw-Hill, New York
12. Angelino G, Invernizzi C, Macchi E (1991) Organic working fluid optimization for space power cycles. In: Angelino G, De Luca L, Sirignano WA (eds) Modern research topics in aerospace propulsion. Springer, New York
13. Curran HM (1981) Use of organic working fluids in Rankine engines. J Energ 5(4):218–223
14. Gaudenzi P (1983) The low-boiling working fluids. Energie Alternative HTE 5(23):229–234 (in Italian)
15. Silvi C (2010) History of steam and electricity generation from solar heat by using flat or almost flat mirrors: research by Italian scientists since the 1800s. Energia Ambiente Innovazione 2:34–47 (in Italian)
16. Angelino G, Gaia M, Macchi E (1984) A review of Italian activity in the field of organic Rankine cycles. In: VDI Berichte 539 – Verein Deutscher Ingenieure. ORC-HP-technology. Working Fluid Problems. Proceedings of the international VFI-seminar, Zürich, 10–12 September 1984, pp 465–482
17. Various Authors (1958) Proceedings of the SRE-OMRE Forum, Held at Los Angeles, California, February 12 and 13, 1958. U.S. Atomic Energy Commission, Technical Information Service Extension, Oak Ridge (TID-7553. NAA-SR-2600)
18. Invernizzi CM (1990) Thermal stability investigation of organic working fluids: an experimental apparatus and some calibration results. La Termotecnica, pp 69–76 (in Italian)
19. Angelino G, Invernizzi CM (1993) Cyclic methylsiloxanes as working fluids for space power cycles. J Sol Energ Eng 115:130–137
20. Invernizzi CM, Pasini A (200) Thermodynamic performances of a new working fluid for power Rankine cycles. La Termotecnica, pp 87–92 (in Italian)
21. Angelino G, Invernizzi CM (2001) Real gas Brayton cycles for organic working fluids. Proc IME J Power Energ 215:27–38
22. Marciniak TJ, Krazinski JL, Bratis JC, Bushby HM, Buyco RH (1981) Comparison of Rankine-cycle power systems: effects of seven working fluids. ANL/CNSV-TM–87, DE82 005599
23. Gaia M, Angelino G, Macchi E, De Heering D, Fabry JP (1984) Experimental results of the organic fluid engine developed for the solar plant of Borj Cedria. Energie Alternative HTE 27(6):31–34 (in Italian)
24. DiPippo R (1979) Geothermal power plants of the Soviet Union – a technical survey of existing and planned installations. Contract EY-76-S-02-4051.A002, Southeastern Massachusetts University, North Dartmouth, MA and Brown University, Providence, RI
25. Cuellar G, Fangzhi Wu, Rosing D (1991) The Nagqu, Tibet, Binary Geothermal Power Plant, at 4500 m above sea level. In: Proceedings of the 13th New Zealand geothermal workshop, Auckland, 1991, pp 57–61
26. Schochet DN (2000) Case histories of small scale geothermal power plants. In: World geothermal congress, Kyushu, Tohoku, 28th May–10th June 2000, pp 2201–2204

27. Angelino G, Bini R, Bombarda P, Gaia M, Girardi P, Lucchi P, Macchi E, Rognoni M, Sabatelli F (1995) One MW binary cycle turbogenerator module made in Europe. In: Proceedings of world geothermal congress, Firenze (Italy), vol 3, pp 2125–2130, 18–31 May
28. Invernizzi C, Bombarda P (1997) Thermodynamic performance of selected HCFS for geothermal applications. Energy 22(9):887–895
29. Riva M, Felix Flohr, Fröba A (2006) New fluid for high temperature applications. In: Proceedings of international refrigeration and air conditioning conference at Purdue, 17–20 July 2006, paper R106, pp 1–8
30. Pernecker G, Uhlig S (2002) Low-enthalpy power generation with ORC-turbogenerator – The Altheim Project, Upper Austria. GHC Bulletin, March 2002, pp 26–30
31. Bombarda P, Gaia M (2006) Geothermal binary plants utilising an innovative non-flammable, azeotropic mixture as working fluid. In: Proceedings of 28th NZ geothermal workshop, November 15–17 2006, Auckland University, 6 pp
32. Gaia M (2006) Turboden ORC systems. In: Electricity generation from enhanced geothermal systems. Doc. 06A01720 - Turboden S.r.l., Strasbourg, 14 September 2006, 23 pp
33. Invernizzi CM, Paolo I, Sandrini R (2011) Biomass combined cycles based on externally fired gas turbines and organic Rankine expanders. Proc IME J Power Energ 215:27–38
34. Obernberger I, Thonhofer P, Reisenhofer E (2002) Description and evaluation of the new 1000 kWe organic Rankine cycle process integrated in the biomass CHP plant in Lienz, Austria. Euroheat Power 10:1–17
35. Pietra C (2008) Thermodynamic optimization of the energy recovery from diesel engines by means of organic Rankine cycles. Ph.D. thesis, Department of Mechanical and Industrial Engineering, University of Brescia (in Italian)
36. Angelino G, Colonna P (1998) Multicomponent working fluids for organic Rankine cycles. Energy 23(6):449–463
37. Chys M, van den Broek M, Vanslambrouck B, De Paepe M (2012) Potential of zeotropic mixtures as working fluids in organic Rankine cycles. Energy 44:623–632
38. Burnside BM (1976) The immiscible liquid binary Rankine cycle. J Mech Eng Sci 18(2):79–86
39. Maloney JD Jr, Robertson RC (1953) Thermodynamic study of ammonia-water heat power cycles. Oak Ridge National Laboratory, CF-53-8-43
40. Ibrahim OM, Klein SA (1996) Absorption power cycles. Energy 21(1):21–27
41. Arima H, Monde M, Mitsutake Y (2003) Heat transfer in pool boiling of ammonia/water mixture. Heat Mass Trans 39:535–543
42. Lu DC, Lee CC (1994) An analytical model of condensation heat transfer of nonazeotropic 1586 refrigerant mixtures in a horizontal tube. In: ASHRAE transactions: symposia OR-94-7-3, 1587 pp 5309–5318
43. Hong EC, Shin JY, Kim MS, Min K, Ro ST (2003) Prediction of forced convective boiling heat transfer coefficient of pure refrigerants and binary refrigerant mixtures inside a horizontal tube. KSME Int J 17(6):935–944
44. Zhang X, He M, Zhang Y (2012) A review of research on the Kalina cycle. Renew Sustain Energ Rev 16:5309–5318
45. Bini R, Manciana E (1996) Organic Rankine cycle turbogenerators for combined heat and power production from biomass. Presented at the third Munich discussion meeting “Energy Conversion from Biomass Fuels – Current Trends and Future Systems”, Münich, 22–23 October 1996. Doc. 96A00412 – Turboden S.r.l., 8 pp